AD-A065 622 NEW MEXICO STATE UNIV LAS CRUCES DEPT OF PHYSICS F/G 4/1
CALCULATION OF THERMAL EMISSION FROM AEROSOLS USING THE DOUBLIN--ETC(U)
NOV 78 A MILLER, R C SHIRKEY, M A SEAGRAVES DAEA18-77-C-0003
UNCLASSIFIED ERADCOM/ASL-TR-0020 NL

1 OF 1
AD A065822

END
DATE FILMED
5-79
DDC

(12) LEVEL II

ASL-TR-0020

AD

Reports Control Symbol
OSD - 1366

AD A065622

CALCULATION OF THERMAL EMISSION FROM AEROSOLS USING THE DOUBLING TECHNIQUE

NOVEMBER 1978

DDC FILE COPY

Prepared by

AUGUST MILLER
RICHARD C. SHIRKEY

Department of Physics
NEW MEXICO STATE UNIVERSITY
LAS CRUCES, NEW MEXICO 88003
and

MARY ANN SEAGRAVES
US Army Atmospheric Sciences Laboratory
WHITE SANDS MISSILE RANGE, NEW MEXICO 88002

US Army Electronics Research and Development Command
Atmospheric Sciences Laboratory
White Sands Missile Range, NM 88002

NOTICES

Disclaimers

The findings in this report are not to be construed as an official Department of the Army position, unless so designated by other authorized documents.

The citation of trade names and names of manufacturers in this report is not to be construed as official Government indorsement or approval of commercial products or services referenced herein.

Disposition

Destroy this report when it is no longer needed. Do not return it to the originator.

SECURITY CLASSIFICATION OF THIS PAGE *(When Data Entered)*

REPORT DOCUMENTATION PAGE

READ INSTRUCTIONS BEFORE COMPLETING FORM

1. REPORT NUMBER: ASL-TR-0020
2. GOVT ACCESSION NO.
3. RECIPIENT'S CATALOG NUMBER

4. TITLE *(and Subtitle)*: CALCULATION OF THERMAL EMISSION FROM AEROSOLS USING THE DOUBLING TECHNIQUE,
5. TYPE OF REPORT & PERIOD COVERED: Research and development Technical Report.
6. PERFORMING ORG. REPORT NUMBER

7. AUTHOR(s): August Miller, Richard C. Shirkey, Mary Ann Seagraves*
8. CONTRACT OR GRANT NUMBER(s): DAEA18-77-C-0003

9. PERFORMING ORGANIZATION NAME AND ADDRESS: Department of Physics, New Mexico State University, Las Cruces, New Mexico 88003
10. PROGRAM ELEMENT, PROJECT, TASK AREA & WORK UNIT NUMBERS: DA Task No. 1L161102B53A SA3

11. CONTROLLING OFFICE NAME AND ADDRESS: US Army Electronics Research and Development Command, Adelphi, MD 20783
12. REPORT DATE: November 1978
13. NUMBER OF PAGES: 60

14. MONITORING AGENCY NAME & ADDRESS *(if different from Controlling Office)*: US Army Atmospheric Sciences Laboratory, White Sands Missile Range, New Mexico 88002
15. SECURITY CLASS. *(of this report)*: UNCLASSIFIED
15a. DECLASSIFICATION/DOWNGRADING SCHEDULE

16. DISTRIBUTION STATEMENT *(of this Report)*

Approved for public release; distribution unlimited.

ERADCOM/ASL

74 p.

17. DISTRIBUTION STATEMENT *(of the abstract entered in Block 20, if different from Report)*

18. SUPPLEMENTARY NOTES

*US Army Atmospheric Sciences Laboratory, White Sands Missile Range, New Mexico 88002

19. KEY WORDS *(Continue on reverse side if necessary and identify by block number)*

Thermal emission
Clouds
Aerosols
Surface effects
Doubling

20. ABSTRACT *(Continue on reverse side if necessary and identify by block number)*

The doubling approach to numerically solving the equation of radiative transfer in a plane-parallel atmosphere is reviewed and extended to include thermal emissions from an ambient medium. The matrix method used is that of Barkstrom and Querfeld and employs the familiar S and T operators to construct a thermal emission operator, E. This new operator is not internally dependent upon the temperature of the layer under consideration, thereby providing a computationally fast method for producing atmospheric models in which thermal emission effects → next page

DD FORM 1 JAN 73 1473 EDITION OF 1 NOV 65 IS OBSOLETE

402005

SECURITY CLASSIFICATION OF THIS PAGE *(When Data Entered)*

20. ABSTRACT (Cont)

cont. are included. The method is further extended to include the effects of the clear air layer below a cloud base and also the effects of emission from the planetary surface.

A computer program using this method is described and results of studies of clouds and smoke are given.

This work was done primarily by the staff at New Mexico State University, Las Cruces, NM, under contract DAEA18-77-C-0003 for the Atmospheric Sciences Laboratory. Contract monitor was Mr. Richard D. H. Low.

SUMMARY

In this report, the authors have demonstrated that the doubling and layer-stacking algorithms used by previous authors for the prediction of reflection and transmission properties of media in which multiple scattering is significant can be extended to the computation of thermal emissions by such a medium. This extension has revealed the existence of an "emission operator" which can be "doubled" in ways closely allied to the doubling of scattering and transmission operators, and which can be utilized for studies of thermal emissions from nonisothermal cloud models. Examples of numerical results obtained by applying these methods demonstrate their applicability to such radiative transfer problems of interest to the Army as those arising from the retrieval of vertical temperature profiles from satellite sounder data and from the determination of the effects of battlefield smoke upon infrared detectors.

CONTENTS

INTRODUCTION

Aerosols in the atmosphere emit thermal radiation with intensities which are functions of their temperature and wavelength. The thermal emission by airborne aerosols is often a significant factor in determining the intensity of infrared radiation transmitted through the atmosphere. For example, in determining vertical temperature profiles from radiance measurements made from satellites, the thermal emission from clouds within the field of view of the instrument must be considered. Another problem of considerable interest to the Army in which aerosol thermal emission may be important is in battlefield scenarios in which smoke clouds may interfere with weapon systems dependent upon infrared viewing devices.

The approach used here in calculating the thermal radiation is analogous to the "doubling" technique used in computing aerosol multiple scattering effects. A summary of the doubling technique is presented, followed by a discussion of its extension to thermal emission calculations. A verification is discussed in which results are compared with some published results of thermal emission from clouds. Also presented are the results of theoretical studies determining the effects of surface radiation passing through a simulated cloud of smoke. The computer program written for the Univac 1108 used in these studies is documented in the appendix. This program is capable of computing water vapor continuum absorption in the 8- to 12-micrometer region using a semiempirical technique [1].

SUMMARY OF THE DOUBLING TECHNIQUE

Consider a horizontally infinite layer of homogeneous aerosol material whose transmittance in the absence of multiple scattering is $e^{-\tau}$, where τ is the optical depth of the layer. Radiation, in the form of a collimated beam of irradiance πF (watts/meter^2), is assumed to be incident from above upon the top of the layer at angle θ_0 and ϕ_0 (see figure 1). It is conventional to represent θ_0 by its cosine, $\mu_0 = \cos \theta_0$, so that directions are specified by μ and ϕ rather than by θ and ϕ. To avoid using negative values of μ, a convention is adopted in which "downward" going radiation is specified by $(-\mu,\phi)$ and "upward" going radiation by (μ,ϕ); thus, the μ's are always regarded as positive numbers. With these conventions, the incident beam direction is specified as $(-\mu_0,\phi_0)$.

Now, let $I(0,\mu,\phi)$ be the radiance (watts/meter^2-steradian) reflected in the direction (μ,ϕ) from the top of the layer. In addition, let the radiance transmitted out from the bottom of the layer (at optical depth τ) be denoted by $I(\tau,-\mu,\phi)$. In the following, the subscript ν is suppressed, although it should be understood unless explicitly stated otherwise.

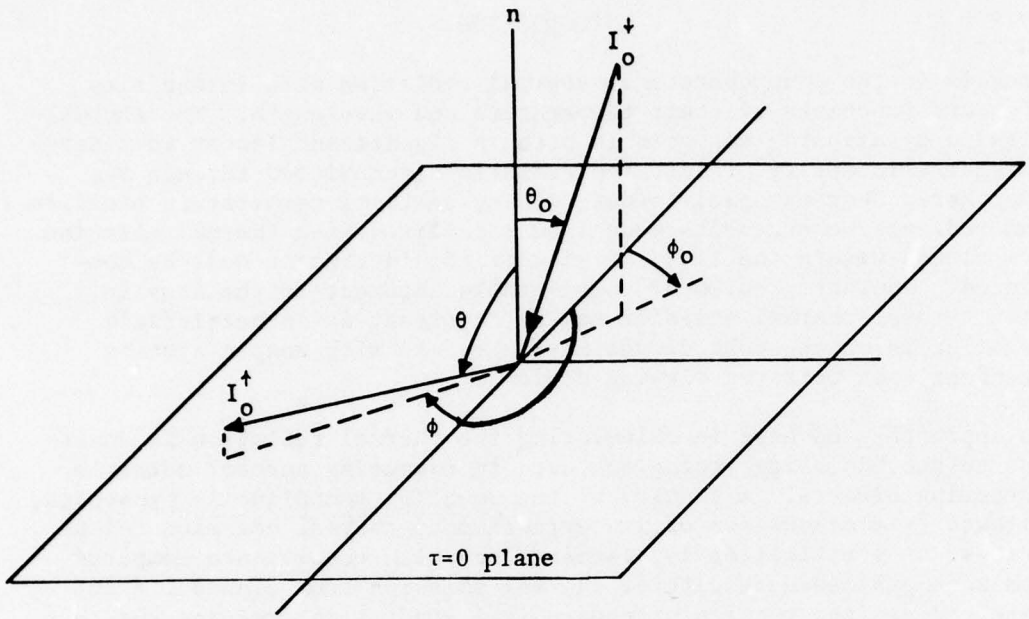

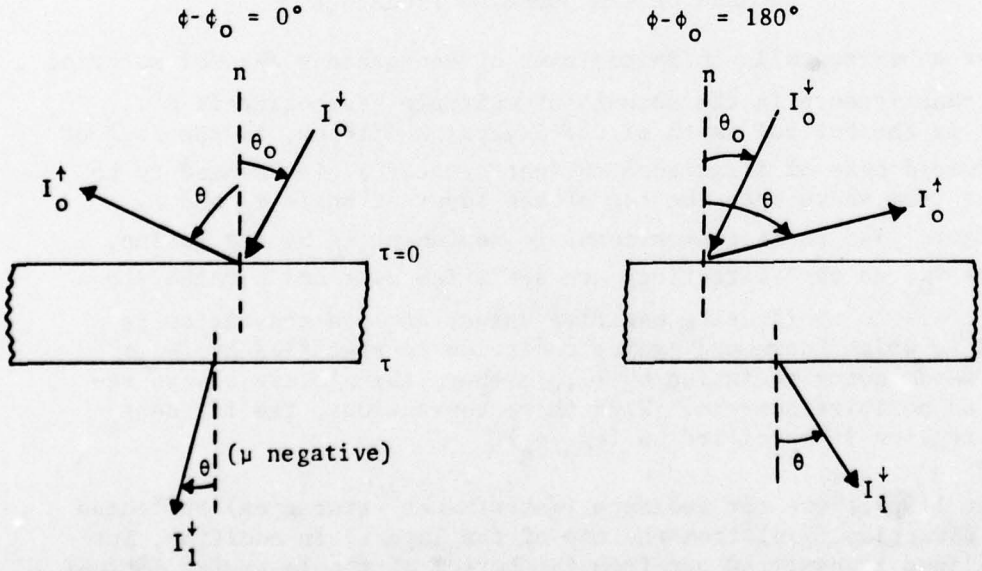

Fig. 1. Angular definitions for multiple scattering calculations (above) and illustration of radiance vectors in the planes $\phi - \phi_o = 0°$ and $\phi - \phi_o = 180°$.

The doubling approach to radiative transfer problems seeks the calculation of two "operators" S and T with the properties:

$$I(0;\mu,\phi) = \frac{1}{4\pi\mu} S(\tau;\mu,\phi;\mu_0,\phi_0)\cdot(\pi F), \tag{1}$$

$$I(\tau;-\mu,\phi) = \frac{1}{4\pi\mu} T(\tau;-\mu,\phi;\mu_0,\phi_0)\cdot(\pi F) + \frac{(\pi F)}{4\pi} e^{-\tau_1/\mu_0} \delta(\mu_0 - \mu)\delta(\phi - \phi_0). \tag{2}$$

The second term of equation (2) represents the attenuated direct beam while the first term represents diffusely transmitted radiance. In subsequent expressions, the factor πF is taken to be unity.

The quantities $S/(4\pi\mu)$ and $T/(4\pi\mu)$ can be regarded as operators whose operands are the incident irradiance. (Alternatively S/μ and T/μ operate on incident radiance.) It may be convenient at times to suppress the μ^{-1} factors by writing $\bar{S}$ for S/μ and $\bar{T}$ for T/μ. The meanings of $\bar{S}$ and $\bar{T}$ can be seen as follows: let $I_0^{\uparrow} = I(0;\mu,\phi)$, the upward intensity at $\tau = 0$; $I_0^{\downarrow} = I(0;-\mu_0,\phi_0)$, the downward intensity at $\tau = 0$, and $I_1^{\downarrow} = I(\tau_1;-\mu,\phi)$, the downward intensity at $\tau = \tau_1$. With these definitions, one can write

$$I_0^{\uparrow} = \bar{S}\, I_0^{\downarrow} \text{ and } I_1^{\downarrow} = \bar{T}\, I_0^{\downarrow}$$

Multiple-scattering calculations using the doubling approach are based upon assumptions that: (1) one can find expressions for S and T which are valid at very small optical depth, that is, under single-scattering conditions, and (2) one can define a procedure for finding the overall scattering and transmission functions for a combination of two layers whose individual S and T functions are already known. To this end, the layer is broken up into a number of layers such that eventual summation of those layers will have the same optical depth as the original layer.

To determine initial values, one starts with a layer of very small optical thickness ($\sim 2^{-20}$) such that the initial S and T values are essentially given by the phase function [2,3]. Once the initial values have been determined, the values of S and T for a layer of twice that starting thickness (optical depth) are found by "stacking" two such layers together. The stacking process is then repeated until the desired final τ value is reached. This general procedure is widely known as the "doubling" method [3,4].

It is assumed that S and T can be expanded in a Fourier series over ϕ and ϕ_0 as follows:†

$$S(\tau;\mu,\phi;\mu_0,\phi_0) = \sum_{m=0}^{N} S^{(m)}(\tau;\mu,\mu_0) \cos\left[m(\phi - \phi_0)\right], \qquad (3)$$

and

$$T(\tau;\mu,\phi;\mu_0,\phi_0) = \sum_{m=0}^{N} T^{(m)}(\tau;\mu,\mu_0) \cos\left[m(\phi - \phi_0)\right]. \qquad (4)$$

Furthermore, since the calculations are numerical (μ and μ_0 are calculated for a discrete number of angles μ_i and μ_j), the operators S and T may be expressed as (operator) matrices with the following notational changes:

$$S^{(m)}(\tau,\mu,\mu_0) \rightarrow S^m_{ij}(\tau) \rightarrow S^m_{ij}\ , \qquad (5)$$

and

$$T^{(m)}(\tau,\mu,\mu_0) \rightarrow T^m_{ij}(\tau) \rightarrow T^m_{ij}\ . \qquad (6)$$

Initial or starting values of S^m_{ij} and T^m_{ij} are found from the following expressions [4]:

$$S^m_{ij}(\tau_0) = (\sigma_i + \sigma_j)^{-1}\left\{1-\exp\left[-(\sigma_i + \sigma_j)\tau_0\right]\right\} P^m_{ij}\ , \qquad (7)$$

$$T^m_{ij}(\tau_0) = (\sigma_i + \sigma_j)^{-1}\left\{\exp(-\sigma_j\tau_0) - \exp(-\sigma_i\tau_0)\right\} \bar{P}^m_{ij}\ , \qquad (8)$$

where

$$\sigma_i \equiv 1/\mu_i \ (\text{and } \sigma_j = 1/\mu_j)\ , \qquad (9)$$

$$P^m_{ij} = \varepsilon^m_0 \sum_{\ell=m}^{N} \tilde{\omega}^m_\ell P^m_{\ell i} P^m_{\ell j}\ , \qquad (10)$$

$$\bar{P}^m_{ij} = \varepsilon^m_0 \sum_{\ell=m}^{N} (-1)^{\ell+m} \tilde{\omega}^m_\ell P^m_{\ell i} P^m_{\ell j}\ , \qquad (11)$$

---

†For problems of azimuthal symmetry, such as the emissions of a blackbody, only the term m = 0 is required.

$$\varepsilon_0^m = 2 - \delta_{0,m}, \tag{12}$$

$$\tilde{\omega}_\ell^m = \frac{(\ell - m)!}{(\ell + m)!}\,\tilde{\omega}_\ell, \tag{13}$$

and $P_{\ell i}^m$ means $P_\ell^m(\mu_i)$, an associated Legendre polynomial evaluated at $\mu = \mu_i$. τ_0 is the optical depth of the initial layer and is taken typically to be 2^{-20}.

For completeness, the $\tilde{\omega}_\ell$ are determined in the single scattering routines (by Gauss-Legendre quadrature) from:

$$\tilde{\omega}_\ell = \frac{2\ell + 1}{2} \int_0^\pi p(\cos\Theta) P_\ell(\cos\Theta) \sin\Theta \, d\Theta \tag{14}$$

in which $p(\cos\Theta)$ is the "phase function" and Θ is the scattering angle:

$$\cos\Theta = \mu\mu' + (1 - \mu^2)^{\frac{1}{2}}(1 - \mu'^2)^{\frac{1}{2}}\cos(\phi - \phi'). \tag{15}$$

Once S_{ij}^m and T_{ij}^m have been calculated for an initial layer, one proceeds to combine two such layers by some "process." The algorithm used here for doing that will be reviewed next. For simplicity, again, all subscripts and functional dependencies will be suppressed: S will represent $S_{ij}^m(\tau)$, $I_0^\downarrow$ will represent $I(0;-\mu_0,\phi_0)$, etc.

Consider two layers identified by the numerals 1 and 2, with 1 being the "upper layer." The upper layer is to be characterized by S_1 and T_1 for illumination from above, and S_1^*, T_1^* for illumination from below. In a similar fashion the lower layer is characterized by S_2, T_2, S_2^*, T_2^* (asymmetries for illumination from above or below are "permitted").

Let

$I_0^\downarrow$ be the downward intensity incident on the top of the upper layer,

$I_0^\uparrow$ be the upward intensity reflected from the top of the upper layer,

and

$I_2^\downarrow$ be the downward intensity at the bottom of the lower layer.

Reference to Figure 2 may be helpful.

Using these definitions, Barkstrom and Querfeld [4] have shown that

$$I_0^{\uparrow} = SI_0^{\downarrow} \quad \text{and} \quad I_2^{\downarrow} = TI_0^{\downarrow},$$

where

$$T = T_2(1 - S_1^* S_2)^{-1} T_1 \tag{16}$$

and

$$S = S_1 + T_1^* S_2 (1 - S_1^* S_2)^{-1} T_1 \ . \tag{17}$$

The above expressions S and T were written in such a way as to permit stacking nonidentical layers, if desired. Note that S_1, T_1, etc., are matrices and that equations such as (17) imply matrix multiplication as well as the Fourier summations indicated in equations (3) and (4).

INCLUSION OF THERMAL EMISSION

For a very thin layer at a temperature t in which single scattering dominates, the emitted intensity can be well approximated by the expression

$$I_{\nu E}^{(\mu)} = (1 - \tilde{\omega}_0)(1 - e^{-\tau_0/\mu}) B_\nu(t), \tag{18}$$

where τ_0 is the optical depth of the layer, $\tilde{\omega}_0$ is the single scattering albedo, and $B_\nu(t)$ is the Planck function at frequency ν. If one regards the intensity emitted by one layer as part of that incident upon another one, it may be possible to assemble an emission operator analogous to S or T. A method for doing that will be described next.

Recall now the two layers utilized in the previous discussion. Ignoring, for the present, any external sources of radiation, one can introduce some additional definitions and quantities. Define

$I_{1E}^{\uparrow}$ as the upward directed thermal intensity found at the top of the upper layer in the absence of the lower layer,

$I_{1E}^{\downarrow}$ as the downward directed thermal emission intensity at the bottom of the upper layer in the absence of the lower one,

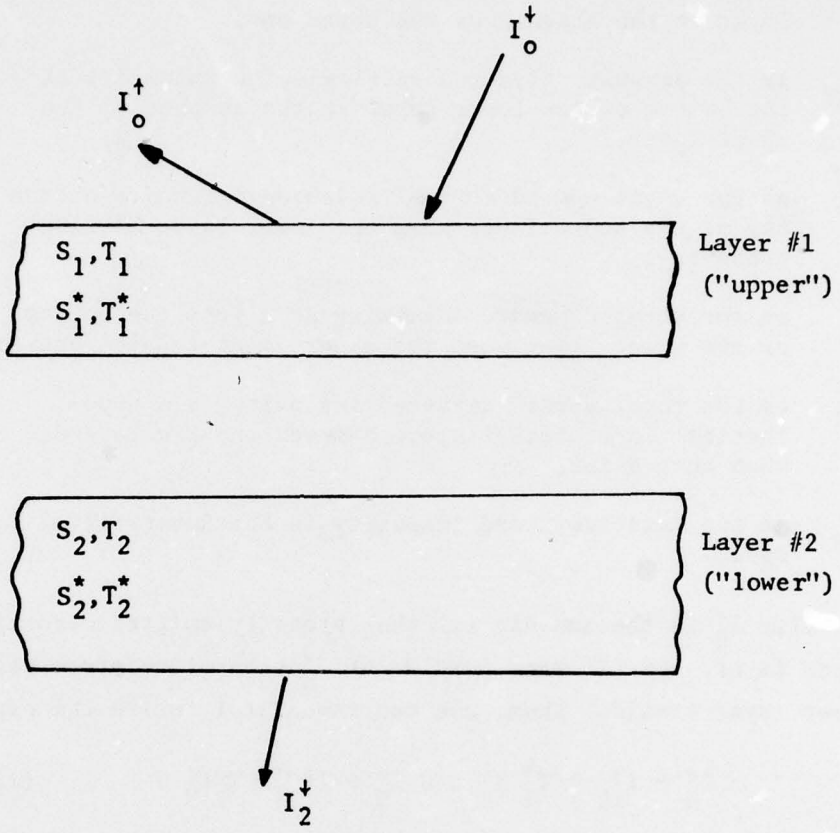

Fig. 2. Geometry and definitions for the stacking algorithms.

$I^{\uparrow}_{2E}$ as the upward self-intensity at the top of the lower layer in the absence of the upper one,

$I^{\downarrow}_{2E}$ as the downward directed self-emission intensity at the bottom of the lower layer in the absence of the upper layer,

$I^{\uparrow}_{E}$ as the total upward thermal emission intensity at the top of the upper layer when the lower layer is also present,

$I^{\downarrow}_{E}$ as the total downward intensity seen from the bottom of the lower layer when the upper layer is also present,

$I^{\uparrow}_{M}$ as the total upward directed intensity in a hypothetical interstitial space between the two layers when both exist,

and

$I^{\downarrow}_{M}$ as the total downward intensity in the interstitial space.

The quantity $I^{\uparrow}_{E}$ is the sum of: (1) the intensity emitted directly by the upper layer, and (2) that portion of $I^{\uparrow}_{M}$ transmitted from below by the upper layer itself. Thus, one can immediately write the expressions:

$$I^{\uparrow}_{E} = I^{\uparrow}_{1E} + T^{*}_{1} I^{\uparrow}_{M} \text{ and } I^{\downarrow}_{E} = I^{\downarrow}_{2E} + T_{2} I^{\downarrow}_{M} . \qquad (19a,b)$$

The quantity $I^{\uparrow}_{M}$ is the sum of $I^{\uparrow}_{2E}$ and that portion of $I^{\downarrow}_{M}$ which is reflected by the lower layer, and $I^{\downarrow}_{M}$ is similarly related to $I^{\downarrow}_{1E}$ and $I^{\uparrow}_{M}$. Therefore,

$$I^{\uparrow}_{M} = I^{\uparrow}_{2E} + S_{2} I^{\downarrow}_{M} \text{ and } I^{\downarrow}_{M} = I^{\downarrow}_{1E} + S^{*}_{1} I^{\uparrow}_{M}. \qquad (20a,b)$$

The last two equations can be combined to give, for example,

$$I^{\downarrow}_{M} = (1 - S^{*}_{1}S_{2})^{-1}[I^{\downarrow}_{1E} + S^{*}_{1} I^{\uparrow}_{2E}]$$

and (21a,b)

$$I^{\uparrow}_{M} = (1 - S^{*}_{1}S_{2})^{-1}[1^{\uparrow}_{2E} + S_{2} I^{\downarrow}_{1E}]$$

which can, in turn, be substituted into equation (19b) to yield:

$$I^{\downarrow}_{E} = I^{\downarrow}_{2E} + (T_{2}QS^{*}_{1})I^{\uparrow}_{2E} + (T_{2}Q)I^{\downarrow}_{1E} , \qquad (22)$$

where Q stands for $(1 - S_1^* S_2)^{-1}$. In a similar way one finds that:

$$I_E^{\uparrow} = I_{1E}^{\uparrow} + (T_1^* S_2 Q) I_{1E}^{\downarrow} + T_1 Q \, I_{2E}^{\uparrow} \, . \tag{23}$$

Equations (22) and (23) provide for combination of the self-emission intensities of two layers whose individual properties are known but not necessarily identical. Thus, they may be used to combine the thermal emissions from two layers which differ from one another in temperature as well as in passive optical properties. Equation (18) may then be used to provide starting values for successive applications of (22) and (23).

The formal procedures derived above may, in principle, be useful for the construction of thermal emission intensities for a cloud composed of nonidentical layers of arbitrarily small thickness and continuously varying temperature. That sort of procedure is not practical, however, because of the inordinately large number of stackings which would be required to attain a total thickness of real interest. To apply equations (22) and (23) to a more realistic case (insofar as numerical computations are concerned), a cloud must be divided into a small number of layers (~ 20) within each of which temperature, droplet size distributions, and other optical parameters are assumed to be uniform. This means that the physical thickness of a layer would be typically too large to permit the use of equation (18) for representing its self-emission levels. The apparent dilemma posed by these contrasting requirements can be resolved by using specialized forms of equations (22) and (23) which lead to the definition of an emission operator, E, analogous to S and T. The existence of the operator E, which is not internally dependent upon the temperature assigned to a layer, allows the use of the doubling equations to establish S, T, and E matrices for a layer of reasonable thickness. Those matrices can then be stored, for example, on magnetic tape, and never need to be recomputed for a given cloud model. One can therefore define a "basic layer" via doubling, and use its S, T, and E operators to examine the effects of larger scale inhomogeneities on thermal emissions.

The procedure described above may, of course, be used to deal with identical layers, in which case the subscripts are irrelevant. If the layers are homogeneous, then the superscript (*) is also immaterial and may be dropped. Under such assumptions $I_{1E}^{\downarrow\uparrow} = I_{2E}^{\downarrow\uparrow}$, and one may simply write I_E in their places, yielding [from eqs. (22) and (23)]

$$I_E^{\downarrow} = [1 + TQ(1 + S)] \, I_E \equiv G I_E \, , \tag{24}$$

where G is a new operator given by $G \equiv 1 + TQ(1 + S)$. It will then

also be evident that $I_E^{\uparrow} = I_E^{\downarrow}$ for an isolated emitting layer.

Equation (24) provides a powerful tool for dealing with self-emission through stacking by eliminating any need to determine the actual values of $I_E^{\uparrow}$ or $I_E^{\downarrow}$ during the early stages of doubling. It will be seen that G is formed from the S and T matrices of the two layers being combined in a certain step. In the next doubling step a new G, say G' will be formed using the *combined* S and T operators which may be called S' and T'. Let I_E be the result of the first doubling step, and I_E' be that of the next step. One has, then,

$$I_E^{\uparrow} = GI_E, \quad \text{and} \quad I_E^{\uparrow\prime} = G'I_E^{\uparrow} . \tag{25a,b}$$

Substitution of equation (25a) into (25b) then yields

$$I_E^{\uparrow\prime} = EI_E , \quad \text{where} \quad E \equiv G'G . \tag{26}$$

The new operator E thus represents an "overall emission operator" which operates on the intensity emitted by the elementary layer used at the beginning. As successive doublings are performed, E may be updated through multiplication on the left by a G which is, itself, fixed by the cumulative S and T operators.

Like S and T, E really carries several parameters and is a short form for its true representation $E_\lambda(\tau,\mu,\mu')$. Similarly $I_E^{\uparrow} = EI_E$ actually stands for:

$$I_E^{\uparrow}(\tau,\mu_i) = \sum_j a_j \, E_{ij}(\tau) I_E(\mu_j) \tag{27}$$

where a_j is the Gauss-Legendre weighting coefficient for abscissa value μ_j.

TREATMENT OF SURFACE EMISSIONS AND THE CLEAR-AIR LAYER BELOW A CLOUD

This section will show the ease with which the layer stacking method can be adapted to a variety of situations. The planetary surface is different from an aerosol layer only in that it is described by different S, T, and E matrices, and the same may be said of the atmospheric layer lying between the cloud and the surface (or above the cloud).

The surface is assumed to be an isotropic emitter and scatterer with

a reflectivity $\tilde{\omega}_s$ and an emissivity $\varepsilon = 1 - \tilde{\omega}_s$. Such a surface can be represented by a scattering matrix $\bar{S}_{ij} = \tilde{\omega}_s \mu_i/(4\pi)$, and a transmission matrix $T_{ij} = 0$.

To reasonable accuracy, a "clear" atmospheric layer can be regarded as neither emitting nor scattering appreciably, but as simply causing attenuation. The appropriate S matrix is zero, and the transmission matrix T_A can be written as

$$(T_A)_{ij} = e^{-\tau_A/\mu_i} \delta_{ij},$$

where τ_A is the optical depth at normal incidence of the atmospheric layer at the wavelength of interest.

By use of the layer stacking algorithm, the surface and clear-air layers can be combined into a single equivalent layer whose transmission matrix T_{AS} and scattering matrix S_{AS} are given by

$$T_{AS} = T_A \tag{28}$$

and

$$S_{AS} = T_A \bar{S} T_A \, . \tag{29}$$

Let $I_S^{\uparrow}$ represent the emitted intensity at the planetary surface and let $I_B^{\uparrow}$ and $I_B^{\downarrow}$ represent the upward and downward intensities at the cloudbase. With these definitions one can then write:

$$I_B^{\uparrow} = T_{AS} I_S^{\uparrow} + S_{AS} I_B^{\downarrow} \tag{30}$$

and

$$I_B^{\downarrow} = I_E^{\downarrow} + S_C I_B^{\uparrow} \, , \tag{31}$$

where S_C is the reflection operator for the cloud. Application of the Barkstrom-Querfeld [4] matrix analysis then yields

$$I_B^{\uparrow} = (1 - S_{AS} S_C)^{-1} [T_A I_S^{\uparrow} + S_{AS} I_E^{\downarrow}] \, , \tag{32a}$$

and

$$I_B^{\downarrow} = [1 + S_C (1 - S_{AS} S_C)^{-1} S_{AS}] I_E^{\downarrow} + S_C (1 - S_{AS} S_C)^{-1} T_{AS} I_S^{\uparrow} \tag{32b}$$

Knowing $I_B^{\uparrow}$ and the transmission operator T_C of the cloud, it is a simple matter to see that the portion of the total upward intensity emitted from the surface which is seen at the top of the cloud is just $[T_C(1 - S_{AS}S_C)^{-1}T_A]I_S^{\uparrow}$, and that $[T_C(1 - S_{AS}S_C)^{-1}S_{AS}]I_E^{\downarrow}$ tells how much of the upward intensity results from downward emission by the cloud, attenuation by the atmospheric layer below the cloud, and subsequent upward transmission through the cloud. In fact, the latter terms also include all multiple reflections between the cloud and the surface.

When all such things are combined, the total upward intensity seen when looking down on the cloud from above is given by

$$I_{up} = I_E^{\uparrow} + \left[T_C(1 - S_{AS}S_C)^{-1}S_{AS}\right]I_E^{\downarrow} + \left[T_C(1 - S_{AS}S_C)^{-1}T_A\right]I_S^{\uparrow}, \quad (33a)$$

$$I_{down} = I_B^{\downarrow}, \quad (33b)$$

wherein $I_E^{\uparrow}$ and $I_E^{\downarrow}$ are the upward and downward self-emission intensities of the existing cloud in the absence of the clear air and the surface itself.

VERIFICATION OF COMPUTER CODE CLEM

The previous formulations have been incorporated into a computer code that is capable of predicting theoretical intensities arising from cloud emissions and/or surface emissions passing through an atmosphere lying between the surface and cloud. CLEM is described fully in the appendix.

Verification of the general soundness of the thermal emission code has been attempted by comparing the results of the new codes with some of the published results of Yamamoto, Tanaka and Kamitani [5], hereafter referred to as YTK, at $\lambda = 10\mu m$. Since the particle distribution used by YTK appeared to be the same as Deirmendjian's [6] cumulus model C.1, that model was used to calculate the phase function. Table 1 presents the results of one such comparison, but it must be realized that the numerical values cited as representing the results of YTK were taken from small published graphs and may not be closer than 5 percent to their actual results. The agreement appears to be quite satisfactory and suggests that the doubling codes contain no major errors.

Results of assuming that thick clouds can be regarded as isothermal (the works of Zdunkowski and Choronenko [7] and of YTK [5], for example) have been examined through a series of computations made at $\lambda = 11.5\mu m$ and using the C.1 cloud model phase function, a variety of layer thicknesses, and a lapse rate of 5°C per kilometer. Each layer was assigned the temperature that would prevail at the center of the layer (the average temperature). In addition several calculations also were made

TABLE 1. COMPARISON OF RESULTS FROM CLEM WITH THOSE OF YTK WITH A SURFACE TEMPERATURE OF 30°C AND A CLOUD TEMPERATURE OF -30°C (λ = 10μm)

Optical Depth	zenith angle(°)	Self-Emission Intensities ($W\ m^{-2}\ str^{-1}\ cm$) Present Calculations	YTK	Total Upward Intensities ($W\ m^{-2}\ str^{-1}\ cm$) Present Calculations	YTK
0.1	0	1.2	1.3	101	101
	70	3.8	5	89	91
1.0	0	11.1	12	79	80
	70	21.6	13	48	46
10	0	31	29	31	29
	70	31	29	31	29

using the isothermal assumption and taking the cloud temperature to be that of the top of the cloud. Table 2 presents the results obtained under the assumptions that surface albedo $\tilde{\omega}_s = 0$, that cloud base temperature is 8°C, that surface temperature is 30°C, and that absorption by the atmosphere below the cloud base is negligible. In the table, the quantities listed as the "apparent temperatures" are the temperatures which would be inferred if the upwardly emitted intensities were assumed to be produced by a blackbody. The data shown in table 2 provide a guide as to the fineness needed in subdividing the layers of a cloud model, and also indicate that the assumption of isothermality (with the cloud top temperature) does not lead to much distortion of the results.

As expected, if the clouds are fairly thin, a substantial portion of the upward radiation arises from the surface, making the apparent temperature quite a bit warmer than the cloud temperature. Therefore, both the "graded temperature" cloud models and the isothermal models give about the same value (the total transmission matrix will be the same whether the cloud is isothermal or not). As the cloud becomes thicker, the discrepancy between the two temperature models increases, but it reaches only about 1°C for a cloud thickness of 1200 m. Also, results of using step sizes of 100 to 200 m yield results very close to those obtained using a 25-m layer thickness. This observation suggests that even if one wants to use a nonisothermal model, a layer thickness of 100 or 200 m is probably small enough.

In general, as the clouds reach optical depths of about 10, the isothermal model will give an apparent temperature which is slightly colder than the cloud top temperature, while a more realistic temperature profile yields a value somewhat (~0.6°C) warmer than the summit tempera-

TABLE 2. COMPARISON OF APPARENT TEMPERATURES FOR ISOTHERMAL AND NONISOTHERMAL CLOUD MODELS.

Cloud Depth (m)	Cloud-Top Temp. (°C)	Optical Depth	Apparent Temperatures* (Lapse rate = 5°C per km) Computation Step Thickness (m) 25	50	100	200	300	Isothermal Single Step to the Given Depth $T = T_{top}$
25	7.875	0.249	26.7	--	--	--	--	--
50	7.75	0.498	23.8	23.8	--	--	--	--
75	7.625	0.748	21.3	--	--	--	--	--
100	7.5	0.997	19.1	19.1	19.1	--	--	19.0
125	7.375	1.246	17.3	--	--	--	--	--
150	7.25	1.495	15.6	15.6	--	--	--	--
175	7.125	1.744	14.2	--	--	--	--	--
200	7.0	1.993	13.0	13.0	13.0	13.1	--	12.7
300	6.50	2.990	9.7	9.7	9.7	--	9.9	--
400	6.00	3.988	7.8	7.8	7.8	7.9	--	7.2
500	5.50	4.984	6.6	6.6	6.6	--	--	--
600	5.0	5.980	--	5.8	5.8	5.9	6.0	--
800	4.0	7.974	--	4.6	4.7	4.7	--	3.9
900	3.50	8.970	--	4.1	4.1	--	4.3	--
1,200	2.0	11.961	--	--	2.6	2.7	2.8	1.8
1,500	0.5	14.951	--	--	1.1	--	1.3	--
1,800	-1.0	17.941	--	--	-0.4	-0.4	-0.2	--

*Surface temperature +30°C, cloud base temperature = +8°C; surface albedo = 0, λ = 11.5μm

ture. In either case, however, the differences between the actual cloud top temperatures and the apparent temperatures are again so small as to be nearly insignificant if $\tau \gtrsim 10$.

One of the major problems to be encountered in temperature retrieval in future automated analyses is that of determining whether any clouds are present and, if so, finding a way to estimate their optical depth. These pieces of information are necessary in assessing the relative contributions to the observed radiance which arises within or below a cloud. It is conceivable that some relevant information might be obtained by making the radiance measurements at more than one infrared wavelength. To see how that might be done, let the earth's surface be assumed to be a blackbody. If no intervening clouds (or only very thin clouds) exist, the inversion of the Planck function for I_{λ_1} and I_{λ_2} should give the same apparent temperature. The same is true if the clouds are very thick since their behavior does become similar to that of a blackbody. If clouds of "intermediate" depth are present, the situation may be different since the transmission and emissive properties of the cloud are wavelength dependent. This line of thought has been examined by comparing apparent temperatures at wavelengths $\lambda_1 = 10\mu m$ and $\lambda_2 = 11.5\mu m$ for several cloud models, thicknesses, and surface temperatures. A few of the results are summarized in figure 3. A comparison of apparent temperatures inferred at wavelengths of 10μm and 11.5μm can provide information of the type suggested above if the cloud base and surface temperatures differ appreciably and if sufficiently precise intensity measurements can be made.

SIMULATED SMOKE STUDIES

Theoretical studies have been made with thermal emission code CLEM to determine the flux received by an idealized detector of variable aperture. The studies were made to determine the effects of surface radiation passing through a simulated cloud produced by white phosphorous munitions. The surface temperature was set at 30°C and 50°C while the cloud temperature was held constant at 100°C.* The wavelengths chosen were 1.06μm and 10.6μm, and the flux into a detector of aperture 180 degrees and 8 degrees was computed. The power into the detector may easily be computed by multiplying the flux by the appropriate surface area of the detector.

The results should be used with care for the following reasons:

1. CLEM does not include a "direct beam" but rather is concerned with multiple scattering effects arising from thermal emissions; there-

---

*This temperature was for white phosphorous smoke, perhaps, unrealistically higher than that of the environment, but that observation does not impair conclusions related to the way in which a smoke of such a high temperature would behave.

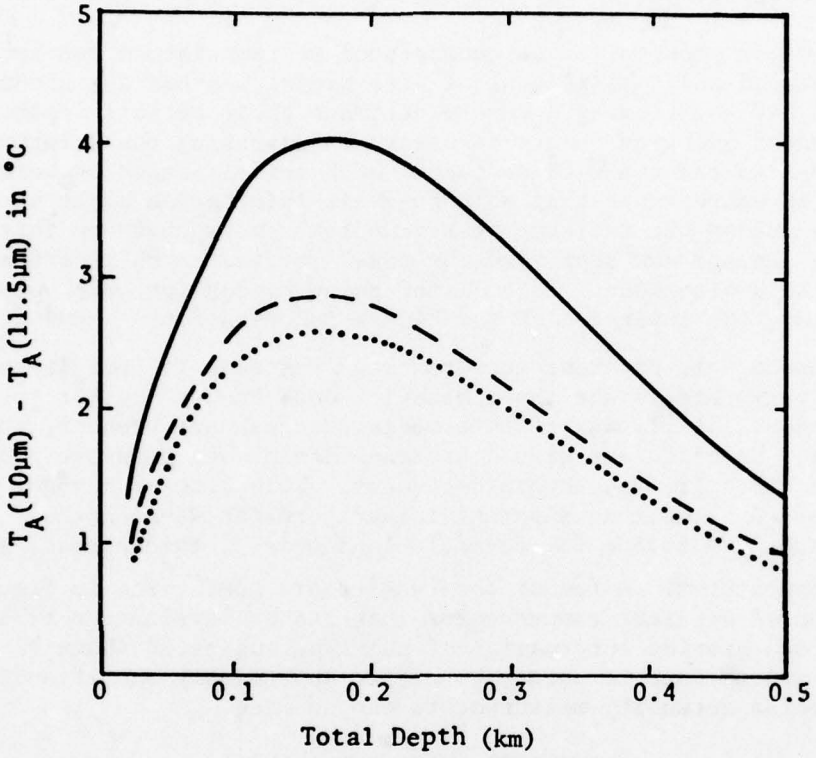

Fig. 3. Differences in apparent temperatures at two distinct wavelengths as a function of cloud depth. The solid curve represents a surface temperature of 30°C and a cloud base temperature of 0°C; for the dashed curve T_s=30°C, T_{CB}=8°C; for the dotted curve T_s=20°C, T_{CB}=0°C. The surface reflectivity was zero, and the cloud model was Deirmendjian's C.1.

fore, the detector is only "seeing" the thermal radiation that is emitted from the surface and/or cloud.

2. The particle distribution [8] may vary with time.

3. In lieu of reliable values for the refractive indices for white phosphorous smoke, the refractive indices of sulfuric acid were used [9].

4. The detector in CLEM is idealized; i.e., reflections off the detector walls and internal noise are not accounted for.

Figures 4 and 5 (a and b) present the ratio of surface emission to surface emission plus cloud emission at wavelengths of 1.06μm and 10.6μm for a reference density of 1.2763×10^3 particles cm^{-3} and at a surface temperature of 30°C and 50°C. The aforementioned density is based on values from Gomez [8]. The bottom abscissas (thickness in kilometers) of figures 4a and b (or figures 5a and b) as may be scaled for other densities by

$$L_{New}(km) = L_{Ref}(km) \frac{N_{Ref}}{N_{New}} = 1.2763 \times 10^3 \frac{L_{Ref}}{N_{New}}, \qquad (34)$$

Where N_{New} is the new density in particles/cm^3, and L_{Ref} is the thickness in km, read from figure 4 or 5.

Thus, if it is assumed that an M15 (STD.C) grenade (0.9 lb fill weight) is used, corresponding to 5.203×10^8 particles, and that the initial burst covers 8 m^3, the average density will be 65.04 particles cm^{-3}. To achieve the same attenuation as the reference density above for $\tau = 0.39(\lambda = 1.06\mu m, T_s = 30°)$, the thickness must be $L_{New}(km) \approx 9.8$.

Figures 6 and 7 present the flux density due to surface emission that has penetrated through the cloud into a 180-degree and 8-degree aperture detector versus thickness. The flux density due to cloud emission may be found by using

$$CF = SF/R - SF, \qquad (35)$$

where CF is the cloud flux density, SF is the surface flux density (from figure 6 or 7), and R is the ratio surface/(surface + cloud) which may be found from either figure 4 or 5. One should take care that the same detector aperture, surface temperature, wavelength, and physical depth are used when computing the cloud flux density by the above formula. Figures 6 and 7 may also be scaled in the same fashion as previously mentioned for the ratio of surface/(surface + cloud) emission.

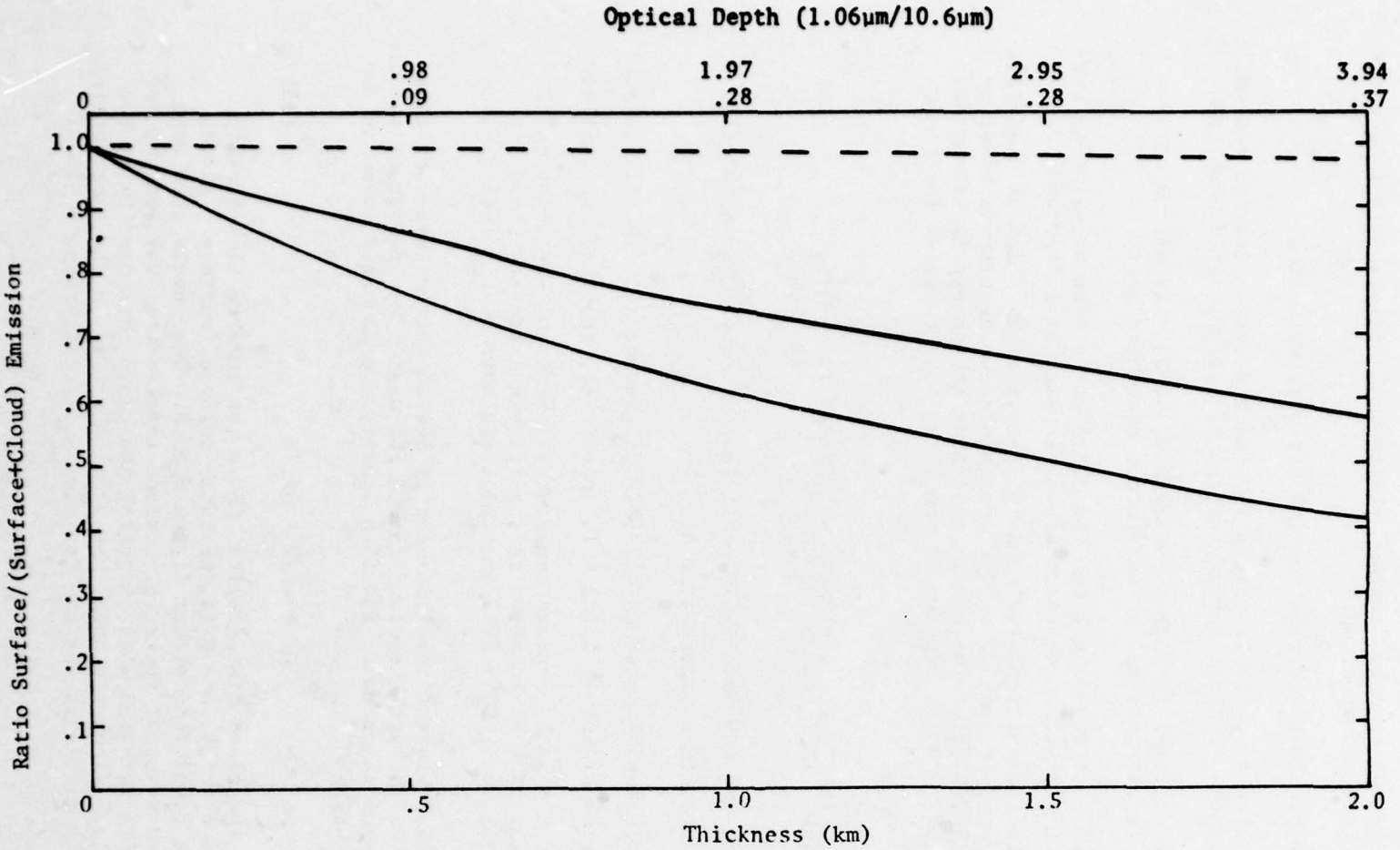

Fig. 4a. Ratio of surface/(surface+cloud) emission for wavelengths of 1.06μm (dashed line) and 10.6μm (solid lines). The dashed line is for a detector aperture of 180° and 8° (the values are coincident); the upper solid curve corresponds to an aperture of 8°. The lower solid curve corresponds to an aperture of 180°. The surface temperature was 50°C; the cloud temperature was 100°C.

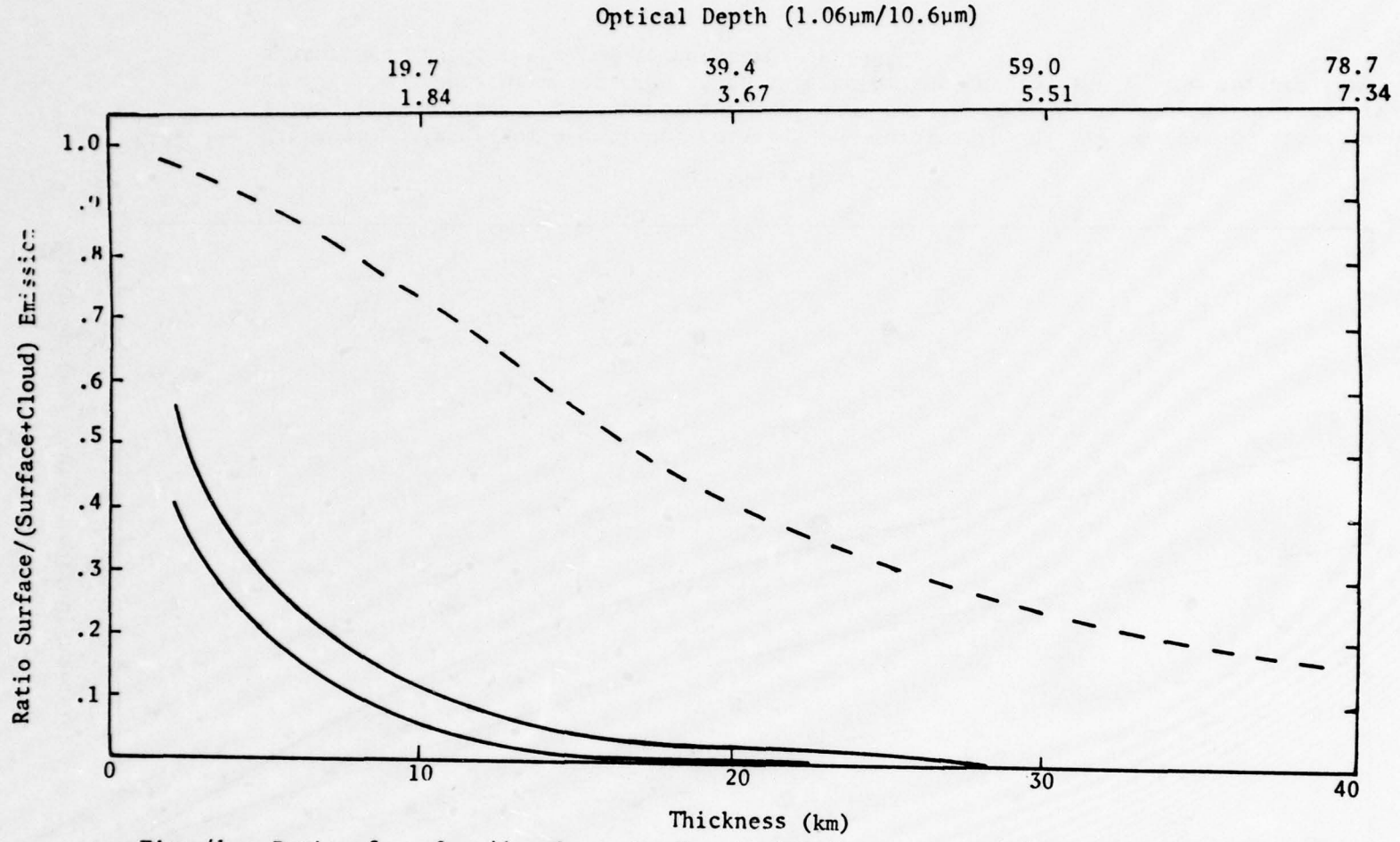

Fig. 4b. Ratio of surface/(surface+cloud) emission for wavelengths of 1.06μm (dashed line) and 10.6μm (solid lines). The dashed line is for a detector aperture of 180° and 8° (the values are coincident); the upper solid curve corresponds to an aperture of 8°. The lower solid curve corresponds to an aperture of 180°. The surface temperature was 50°C; the cloud temperature was 100°C.

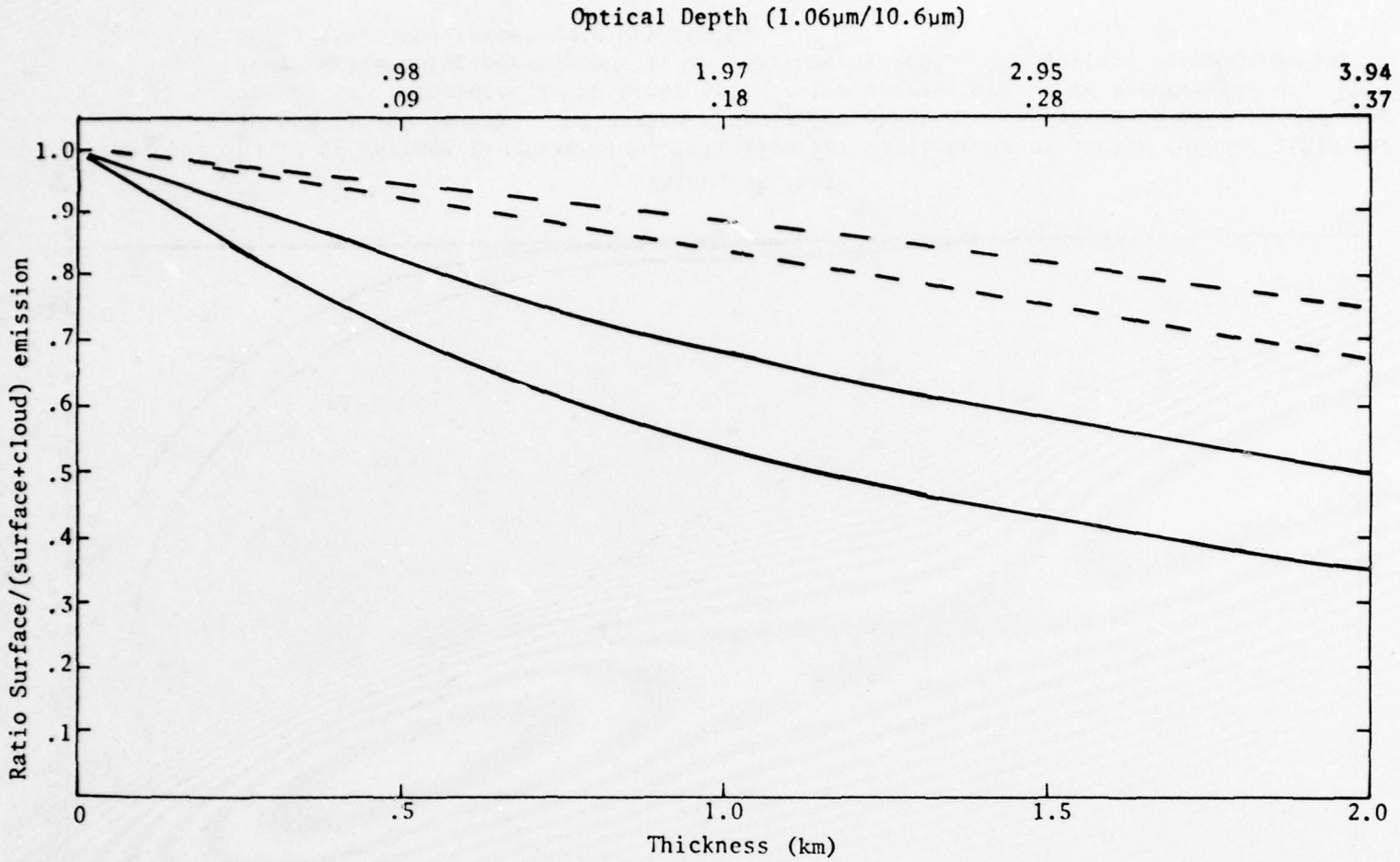

Fig. 5a. Ratio of surface/(surface+cloud) emission for wavelengths of 1.06μm (dashed lines) and 10.6μm (solid lines). The upper curve of each set corresponds to a detector aperture of 8°; the lower curve corresponds to a detector aperture of 180°. The surface temperature was 30°C; the cloud temperature was 100°C.

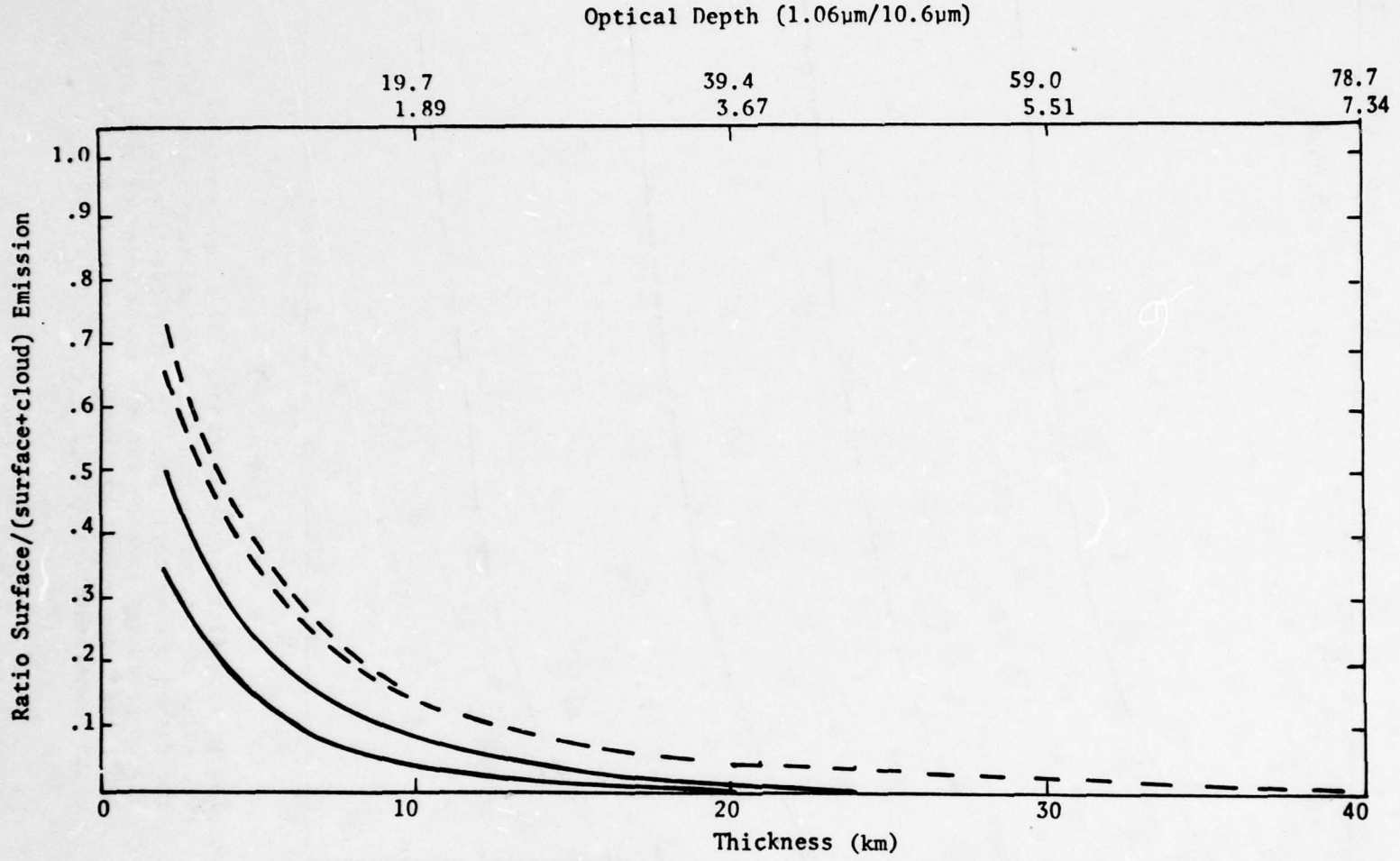

Fig. 5b. Ratio of surface/(surface+cloud) emission for wavelengths of 1.06μm (dashed lines) and 10.6μm (solid lines). The upper curve of each set corresponds to a detector aperture of 8°; the lower curve corresponds to a detector aperture of 180°. The surface temperature was 30°C; the cloud temperature was 100°C.

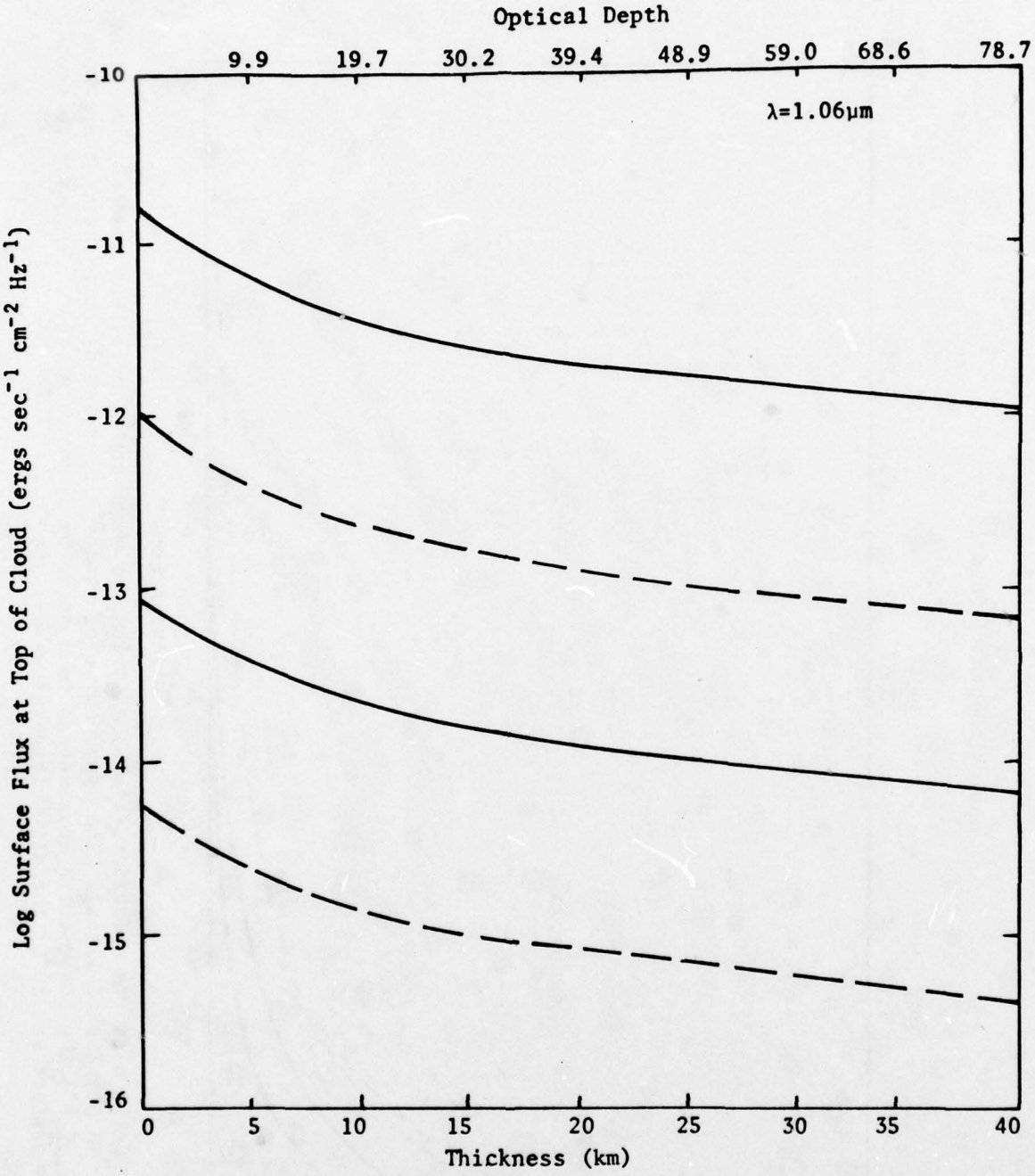

Fig. 6. Log surface flux versus thickness for a wavelength of 1.06μm. The solid curves correspond to a surface temperature of 50°C; the dashed curves correspond to a surface temperature of 30°C. The upper curves in each set are for a detector aperture of 180°; the lower curves are for an aperture of 8°. The cloud temperature was 100°C.

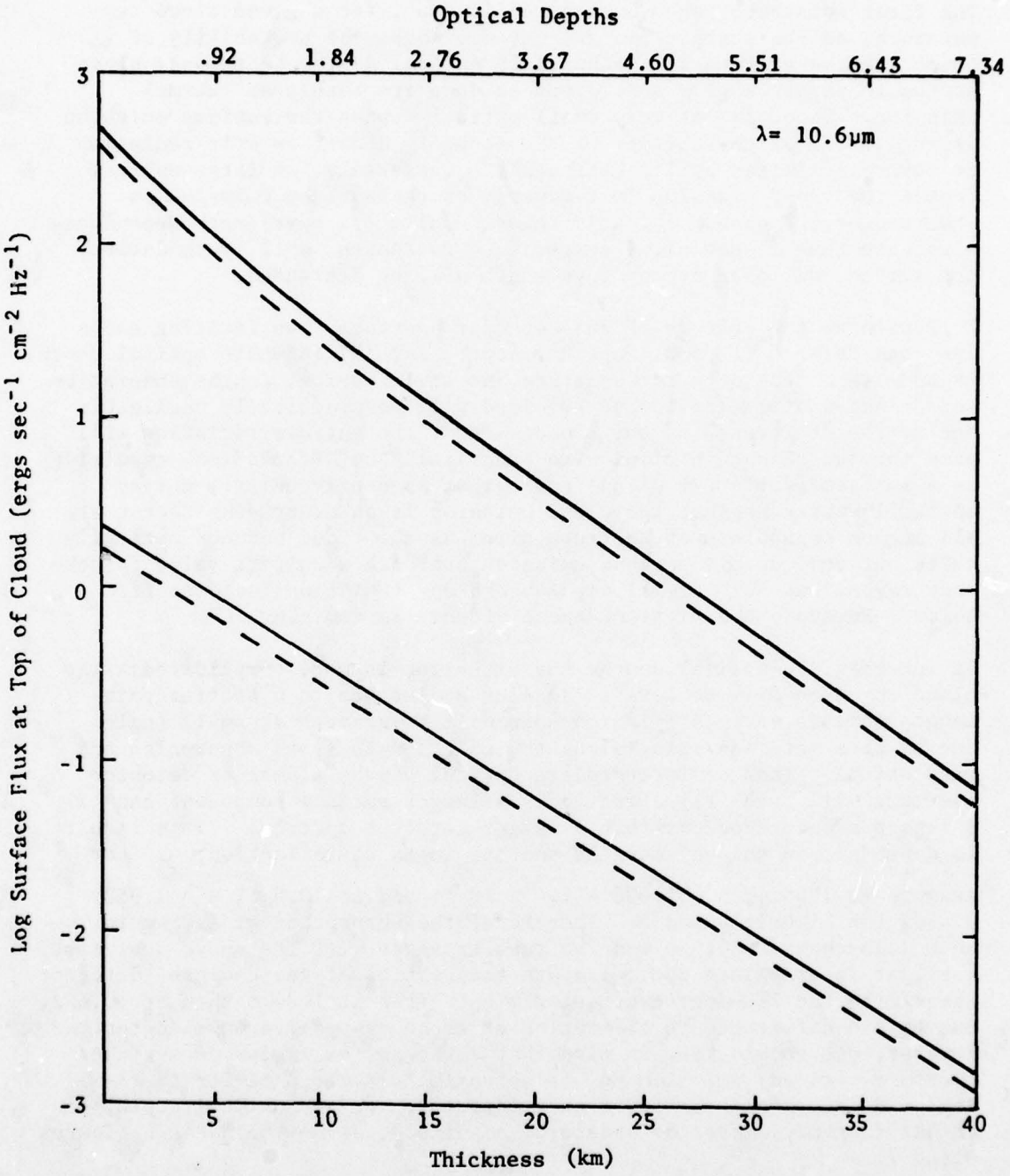

Fig. 7. Log surface flux versus thickness for a wavelength of 10.6μm. The solid curves correspond to a surface temperature of 50°C; the dashed curves correspond to a surface temperature of 30°C. The upper curves in each set are for a detector aperture of 180°; the lower curves are for an aperture of 8°. The cloud temperature was 100°C.

The first point that should be noted is that, for a given cloud temperature, as the surface temperature decreases the probability of detecting the surface at intermediate optical depths decreases, since as the temperature of a body drops so does its resultant thermal emission. Secondly, at very small optical depths the surface emission is recovered, as the ability of the cloud to absorb or emit radiation is severely limited by its "thinness." Conversely, at large optical depths the cloud emission is recovered as the surface emission is absorbed by the cloud. Clearly these results are wavelength dependent. Also note that as the cloud temperature increases, ability to detect the surface emission at any wavelength will be decreased.

In examining the effects of the detector aperture, two limiting cases are considered: (1) small optical depth, and (2) infinite optical depth. Regardless of the detector aperture, at small optical depths absorption and emission of radiation by the cloud will be practically negligible due to the "thinness" of the cloud. Thus, the surface radiation will pass through this thin cloud with practically no attenuation, resulting in a surface/(surface + cloud) ratio that is nearly unity. For an optically thick medium, the cloud emission is an overriding factor at all angles regardless of aperture size; as the cloud becomes optically thick not only does the cloud emission approach a uniform value (blackbody radiation) but it will also absorb any radiation incident from below. However, the first of these effects is dominant.

At intermediate optical depths the situation is more complicated: the cloud emission will be less at smaller angles due to a shorter path length and the surface emission seen will be greater at small angles due to less material lying along the path length (less absorption and scattering). Thus at intermediate optical depths a smaller detector aperture will "see" (1) effectively a larger surface component and (2) a lesser cloud component than a larger detector aperture. This result is dependent on the wavelengths and the index of refraction, n. For example at 1.06μm, $n = 1.426 - 1.4 \times 10^{-6} i$ and at 10.6μm, $n = 1.953 - 0.468i$ for figures 4 and 5. Therefore, the absorption at 1.06μm is much less than at 10.6μm and the results agree with the above analysis, i.e., at intermediate optical depth the results of the 8-degree detector agree with the 180-degree detector much better at 1.06μm than at 10.6μm, due to the difference in absorption at these respective wavelengths. However, one should keep in mind that although the ratios of surface/(surface + cloud) emission may be approximately the same for the 8-degree detector and the 180-degree detector, for any optical depth, the actual flux may differ by orders of magnitude, as may be seen in figures 6 and 7.

In summary, at small optical depths, the surface may be detected with little problem at any wavelength, while at large optical depth there is little chance of detecting emission from the surface. At intermediate optical depth, the ability to detect surface emission is highly dependent upon the index of refraction of the medium under consideration. Also, the thermal emission arising from the cloud must be accounted for.

REFERENCES

1. Roberts, R. E., J. E. A. Selby, and L. M. Biberman, 1976, "Infrared Continuum Absorption by Atmospheric Water Vapor in the 8-12μm Window," Applied Optics, 14:2085-2090.

2. Chandrasekhar, S., 1960, Radiative Transfer. New York, Dover Publishing, Inc., 393 pp.

3. Hansen, J. E., 1969, "Radiative Transfer by Doubling Very Thin Layers," Astrophysics Journal, 155:565-573.

4. Barkstrom, B. R., and C. W. Querfeld, 1975, "Concerning the Effect of Anisotropic Scattering and Finite Depth on the Distribution of Solar Radiation in Snow," Journal of Glaciology, 14:107-124.

5. Yamamoto, G., M. Tanaka, and K. Kamitani, 1966, "Radiative Transfer in Water Clouds in the 10-Micron Window Region," Journal of the Atmospheric Sciences, 23:305-313.

6. Deirmendjian, D., 1969, Electromagnetic Scattering on Spherical Polydispersions, American Elsevier, New York.

7. Zdunkowski, W. G., and I. Choronenko, 1969, "Incomplete Blackness of Clouds in the Infrared Spectrum," Beiträge zur Physik der Atmosphäre, 42:206-224.

8. Gomez, R. B., private communication, May 1977, provided a copy of a document entitled: "The Effectiveness of Obscuring Smokes," by Morris C. Johnson, Paul D. Forney and Thomas J. Dolce, an unpublished ORG [JTCG/ME] report dated September 1972, Edgewood Arsenal, Maryland. (This document was also referred to as SOM.)

9. Palmer, K. F., and D. Williams, 1975, "Optical Constants of Sulfuric Acid: Application to the Clouds of Venus?" Applied Optics, 14:208.

APPENDIX

DESCRIPTION OF CLOUD EMISSION COMPUTER CODE CLEM

CLEM is a thermal emission routine that will calculate intensities, via the doubling method, at the top and bottom of a cloud base due to surface emission and cloud emission. Because CLEM was constructed to operate at infrared wavelengths, no direct beam is included. Treatment of continuum absorption by water vapor for saturated layers is available in the program. The following description is aimed at understanding how the program operates, what arrays are used for what variables, and a general description of the computer code. It should be noted that layers are added to the bottom of the stack instead of the top within the program.

Subroutine EMGUST is called to determine the Gauss-Legendre weights [W(I)] and abscissas [EMU(I)] by Newton-Ralphson iteration for the interval (-1,1). After the return to MAIN the abscissas are shifted into the interval 0,1 and SIG(I) = $1/\mu_i$, and W(I) = W(I)/μ_i, where $\mu_i = \cos\theta_i$ are calculated and stored along with the angles themselves [EMO(I)]. As the index I increases, θ will go from approximately 90 degrees to approximately 0 degrees ($\mu = 0 \rightarrow 1$). The next read is: NLYRS, the number of layers of thickness THICK (in kilometers); ALBS, the surface albedo; TMSC, the temperature of the surface in degrees Centigrade; MODEL: 0 → skip subroutine VAPOR, 1 → AFCRL tropical atmospheric model, 2 → AFCRL midlatitude summer model, 3 → AFCRL midlatitude winter model, 4 → 1962 US standard atmosphere model, 99 → cloud saturation only; HEIGHT, the cloud base height in kilometers; PUNCH, if less than one, punch output for the plotter; TAUR(I) for I = 1, NLYRS, temperature in degrees Centigrade of layer number I. This previous data must be user supplied, whereas all subsequent data are produced by the Mie program. The next read is: NWAVE, the number of wavelengths under consideration; NN, the number of Legendre coefficients; GNU, the wavenumber under consideration; and CT, the extinction coefficient.

The next read is for the Legendre coefficients [OL(I)], where I = 1,NN and NN equals the number of coefficients (which cannot exceed 32). The phase function should be normalized so that the first Legendre coefficient OL(1) is equal to the single-scattering albedo $\tilde{\omega}_o$. The next call is to VAPOR, which will set up the proper atmosphere (below the cloud base) according to whether MODEL is equal to 1, 2, 3, or 4, and return TAUA the optical depth of the atmosphere below the cloud base adjusted for water vapor absorption at temperature. Next compute TMPS, the Kelvin temperature of the surface and TAUI, the optical thickness of the basic layer (cloud). Then a few manipulations are performed to determine the number of doublings (NTI) necessary to get to the final optical depth.

Subroutine CLSTK is a doubling routine, which basically will double up to the basic cloud (or layer) thickness and determine the total (for this layer) scattering, transmission, and the multiple scattering operators for thermal emissions. Note that CLSTK is not concerned with the atmosphere or surface, but only with the cloud (basic layer). Unless otherwise noted, here and elsewhere the incident angles are labeled J and the exit angles are I. Computations are performed to determine the Legendre polynomials [PL(I,J)]; find the beginning layer thickness [TAU]; find the exponential attenuation at TAU for a given incident angle [ETS(I)]; set F(I,J,1) equal to the identity matrix; find the phase function needed for initial computation of the scattering matrix [negative argument, ends up in P(I,J)] and for the transmission matrix [positive argument, ends up in R(I,J)]; finally calculate the initial scattering and transmission matrices [S(I,J,1) and T(I,J,1)] and add in the exponential term on the diagonal to T(I,J,1). As NEWOLD = ϕ, in this call, now proceed to double the appropriate matrices.

The basic doubling loop for CLSTK is loop 26, and the general format is to calculate the appropriate matrices from the previous ones. This calculation is accomplished by indexing S, T, and F (the scattering, transmission and "thermal" operators) with a third subscript, equal to 1 or 2. On the first pass LA = 1, LB = 2; and on subsequent passes their order is interchanged, as the "future" operator is calculated from the previous one.

Thus the first operation that is performed is: $Q = 1 - S_1 S_2$. The Q matrix is then inverted by either (1) taking the first two terms of a MacLaurin expansion (if Q is small and IFAST has been set $\neq 0$), or (2) calling a Gauss-Jordan matrix inversion routine [EMINV]. In either case Q is returned as $(1 - S_1 S_2)^{-1}$. Starting now at label 14 compute $A(I,J) = (1 - S_1 S_2)^{-1} T_1$ and $B(I,J) = T_1 S_2$. The appropriate matrices are now available to determine the "new," or doubled, values for S and T. Thus (note the third subscript here) $T(I,J,\underline{2}) = T_2(1 - S_1 S_2)^{-1} T_1$, the "new" value of T, and $S(I,J,\underline{2}) = S_1 + T_1 S_2 (1 - S_1 S_2)^{-1} T_1$, the "new" value of S. The rest of this do loop (26) is used to compute the "new" thermal emission operator F. Thus, first compute C(I,J) = 1 + S, where S is the original scattering matrix, not the "new" or doubled value. At this point, also drop the subscripts on T and S (i.e., $T_1 = T$, $S_1 = S$, etc.); as for a homogeneous layer, thermal emission is isotropic. Next compute $Q1(I,J) = (1 - SS)^{-1}(1 + S)$ and then $G(I,J) = 1 + T(1 - SS)^{-1}(1 + S)$. The final part of this loop (26) computes the new or doubled value of the thermal emission operator: $F(I,J,\underline{2}) = [1 + T(1 - SS)^{-1}(1 + S)] \times F(I,J,1)$, where one should recall that on

the first pass F(I,J,1) ≡ 1. The optical depth is then incremented and the doubling continues until the final optical depth of the basic layer is reached.

After the doubling loop is complete, the final thermal emission matrix operator for a homogeneous layer is now stored in F; S and T still have their usual meanings. Subsequently the subroutine will return values to MAIN for the final (doubled) basic layer via a switch and equivalence statement. Thus the returned values for the basic layer are: A → current "doubled" value of S; B → current "doubled" value of T; and P → current "doubled" value of F. The switch determines that the correct values, and not the previous values, are placed in the proper arrays.

After the return to MAIN the albedo for single scattering for the cloud is saved in ALBC. Now if MODEL = 0 VAPOR is effectively bypassed. If not, set TMP equal to the Kelvin temperature of the cloud and call VAPOR, which (last argument = 99) will change the physical depth of the cloud (rather than the optical depth) to account for absorption by water vapor molecules at 100 percent relative humidity. TMP is returned as an additional extinction coefficient which is used to reduce the thickness [TAUT] of the basic layer.

Now OL(I) and Q1(I,1) are computed as the thermal emission due to a blackbody whose emission is 1 and albedo of single scattering is Ø. (Recall that here P ≡ F.) The surface emission (ESURF) is then calculated by calling PLANCK, which for a given wavenumber (GNU) and temperature (TMPS) will return the blackbody emission as BNUS. Note that at the ground surface tau is considered infinite. The blackbody radiation of a cloud of infinite optical thickness (ECLOUD) is then found by the same procedure as described for the surface emission, but at the temperature for our first basic slab [TAUR(1) + 273.16]. The next loop (28) first finds the interpolated thermal intensities of an infinitely thick cloud whose blackbody emission is 1, for 0 degrees → 75 degrees in 5-degree increments. This quantity is returned from the interpolation routine [EMNTRP] as ALBUP(1). The true thermal emission due to the cloud at the appropriate temperature and optical depth is calculated and stored in Q1(I,5), ETS(I), and Q1(I,6). Note that here OL = $F \cdot (1 - e^{-\tau/\mu})$ and ECLOUD = $(1 - \tilde{\omega}_{o_c})B_\nu(T_C)$. Within the same loop the combined scattering matrix for transmission (downward) by the atmosphere, scattering by the surface, and retransmission (upward) by the atmosphere as seen at cloud base (S_{AS}) is calculated and stored in PL(I,J). Subsequent to this, but still within the same loop, there is an array transfer; matrices G, BS, and AS are set equal to A (combined value of S, the scattering matrix for the basic layer); matrices AT, BT, and Q2 are set equal to B (combined value of T, the transmission operator for the basic layer).

Next, subroutine EMPR6Ø is called, which essentially processes data,

includes surface effects, and writes output for the first layer, including surface and atmospheric effects. First, intensity due to the surface as seen at the cloud base is calculated [EYUP(I) = $(1 - \tilde{\omega}_{o_S})$ $B(T_S)T_A$], and the matrix Q becomes $(1 - S_{AS}S_C)$, which is then inverted by EMINV and Q is returned as $(1 - S_{AS}S_C)^{-1}$. New matrices B = $T_C(1 - S_{AS}S_C)^{-1}$ and P = $S_C(1 - S_{AS}S_C)^{-1}$ are then calculated, and subsequently the matrix R = $T_C(1 - S_{AS}S_C)^{-1}S_{AS}$ is also computed. At this point, note that if $\tilde{\omega}_{o_s}$ = 0 then the scattering operator goes to zero and thus so does S_{AS}, the combined transmission-scattering-retransmission operator for the atmosphere and surface. In this case P → S_c B → T_c, R → ∅, and PL → ∅, where an appropriate switch has been incorporated in the program. The subscript c represents the cloud. Next Q1(I,7) = $T_c(1 - S_{AS}S_c)^{-1}T_A I_S^{\uparrow}$, the upward intensity due to the surface, looking down on the cloud from above is found. Note that EYUP = $T_A I_S^{\uparrow}$ already has the atmospheric attenuation included. Q1(I,11) = $T_c(1 - S_{AS}S_c)^{-1}S_{AS}I_E^{\uparrow}$ + $I_E^{\downarrow}$, the downward thermal emission due to the cloud, which has been multiply reflected and transmitted by the cloud, atmosphere, and surface is computed. Then the matrix R = $S_C(1 - S_{AS}S_C)^{-1}S_{AS}$ is calculated.

The final intensities at the Gauss-Legendre angles are then calculated:

Q1(I,10) = P×EYUP = $S_C(1-S_{AS}S_C)^{-1}T_A I_S^{\uparrow}$: the surface emission in the downward direction as seen at the cloud base

Q1(I,8) = R×$Q1_5$+$Q1_5$=$S_C(1-S_{AS}S_C)^{-1}S_{AS}I_E^{\downarrow}+I_E^{\downarrow}$: the cloud emission in the downward direction as seen at the cloud base

Q1(I,9) = $Q1_8$+$Q1_{10}$=$(1-S_{AS}S_C)^{-1}[S_C T_A I_S^{\uparrow}+S_C S_{AS} I_E^{\downarrow}]+I_E^{\uparrow}$: the total emission in the downward direction as seen at the cloud base

Q1(I,12) = $Q1_7$+$Q1_{11}$=$T_C(1-S_{AS}S_C)^{-1}T_A I_S^{\uparrow}+T_C(1-S_{AS}S_C)^{-1}S_{AS}I_E^{\uparrow}+I_E^{\downarrow}$: the total emission in the upward direction as seen at the cloud top

and also

$Q1\ (I,13) = Q1_7/ESURF = T_C(1-S_{AS}S_C)^{-1}T_A I_S^{\uparrow}/[(1-\tilde{\omega}_{o_s})B_\nu(T_S)]$

$Q1(I,14) = T_{Apparent}$.

In summary then the Q1 matrices are as follows:

$Q1_7$ → upward intensity at TOC due to the surface emission.

$Q1_{11}$ → upward intensity at TOC due to downward emission by the cloud.

$Q1_{10}$ → downward intensity at BOC due to the surface emission.

$Q1_8$ → the downward intensity at BOC due to multiply scattered cloud emission plus the downward cloud emission.

$Q1_9$ → the total downward intensity of BOC.

$Q1_{12}$ → the total upward intensity at TOC.

The last part of this routine simply interpolates [via EMNTRP] the Q1's and returns them as ALBUP's, and then prints the necessary quantities. There is a one-to-one correspondence between Q1 and ALBUP for the second index of Q1.

Now return to MAIN where the "stacking" loop is entered and some matrices are rearranged: $Q1(I,3) = Q1(I,4)$ = thermal emission matrix for the next layer = $G(1 - e^{-\tau/\mu})(1 - \tilde{\omega}_{o_c})B_\nu(T_c)$; $Q1(I,1) = Q1(I,2)$, the thermal emission matrix for the previous layer; A = P = S; B = R = T; AS = BS = G; AT = BT = T. Note that only on this first pass does A = P, etc. In subsequent passes $S_1 \neq S_2$ and therefore A ≠ P, etc. Next find the total thickness (kilometers) of the "final" layer [TAUU], and after calling VAPOR, the thickness of the new upper layer (kilometer) [TAUL]. From here go to subroutine ADDER.

ADDER basically will combine a "basic" layer, with the previous layer (note that the previous layer means from the cloud base upward, i.e., the atmosphere and surface are not included here, but rather in EMPR6Ø). ADDER will also combine homogeneous and inhomogeneous layers.

The first loop in ADDER essentially rearranges variables:

EYUPU = $I_{1E}^{\uparrow}$; EYDNU = $I_{1E}^{\downarrow}$; EYUPL = $I_{2E}^{\uparrow}$; EYDNL = $I_{2E}^{\downarrow}$; where the subscript 1 denotes the previous layer and 2 denotes the upper, or new, layer.

Also, transfer $C=S_1^*$; $D=T_1^*$; $E=S_2$; $F=T_2$; $G=S_2^*$; $H=T_2^*$: note that when ADDER is called $A = S_1$ and $B = T_1$. Next find Q and invert it so that $Q = (1 - S_1^*S_2)^{-1}$. Then set Q1 = Q and $R = (1 - S_1^*S_2)^{-1}T_1$. Subsequently, $P = S_2(1 - S_1^*S_2)^{-1}T_1$; $AT = T_2(1 - S_1^*S_2)^{-1}T_1$ (which is the "new" T); and $AS = T_1^*S_2(1 - S_1^*S_2)^{-1}T_1 + S_1$ (which is the "new" S). Now if INHOMO = 2, then the layers are inhomogeneous and $S_1^* \neq S_1$, etc; otherwise, BS = AS and BT = AT. If the layers are inhomogeneous, the following occurs: $Q = (1 - S_2S_1^*)^{-1}$; $R = (1 - S_2S_1^*)^{-1}T_2^*$; $BT = T_1^*(1 - S_2S_1^*)^{-1}T_2^*$ (the new T^*); $P = S_1^*(1 - S_2S_1^*)^{-1}T_2^*$; $BS = S_2^* + T_2S_1^*(1 - S_2S_1^*)^{-1}T_2^*$ (the new S^*). From here the rest of the routine is concerned with finding the cloud intensities for the combined layers. Thus, $A = S_2(1 - S_1^*S_2)^{-1}$; $B = T_2(1 - S_1^*S_2)^{-1}$; $G = T_1^*S_2(1 - S_1^*S_2)^{-1}$; $E = T_2(1 - S_1^*S_2)^{-1}S_1^*$. Now INHOMO = 0 implies that the two layers are at the same temperature and thus will have the same blackbody emission. If this is not so, $H = T_1^*S_2(1 - S_1^*S_2)^{-1}S_1^* + T_1^*$ is calculated. Next the resultant thermal emission intensity in the downward direction is found: $Q1(I,6) = T_2(1 - S_1^*S_2)^{-1}S_1^*I_{2E}^{\uparrow} + T_2(1 - S_1^*S_2)^{-1}I_{1E}^{\downarrow} + I_{2E}^{\downarrow}$, and if the layers are at the same temperature $Q1(I,5) = Q1(I,6)$; else $Q1(I,5) = T_1^*S_2(1 - S_1^*S_2)^{-1}I_{1E}^{\downarrow} + [T_1^*S_2(1 - S_1^*S_2)^{-1}S_1^* + T_1^*]I_{2E}^{\uparrow} + I_{1E}^{\uparrow}$, the resultant thermal emission intensity in the upward direction. Now return to MAIN.

The return to MAIN is still in the doubling loop and processes are continued until the final optical depth is reached. The program will loop back to 502 CONTINUE if the number of wavelengths is greater than one; in this case new, values for NN, GNU, CT, and the Legendre coefficients must be supplied for every new wavelength.

INPUT FOR CLEM

CARD 1

Input Symbols
NLYRS, THICK, ALBS, TMSC
[FORMAT(I5, 3F10.6)]

NLYRS = number of layers of thickness THICK
THICK = thickness of individual layers
ALBS = surface albedo
TMSC = surface temperature (°C)

CARD 2

Input Symbols

MODEL, HEIGHT, PUNCH
[FORMAT(I5, 2F10.6)]

MODEL = 0 for no atmospheric continuum absorption
1 for AFGL Tropical atmospheric model
2 for AFGL Midlatitude summer atmospheric model
3 for AFGL Midlatitude winter atmospheric model
4 for US 1962 standard atmospheric model
HEIGHT = height of atmosphere ($\leq$ 9 km)
PUNCH = if $\leq$ zero, punch "retrieved" temperatures at preselected angles after each doubling.

CARD 3

Input Symbols

TAUR(I), I = 1, NLYRS
[FORMAT(10F8.2)]

TAUR ( ) = true temperature of individual layers (°C)

CARD 4

Input Symbols

NWAVE
[FORMAT(I5)]

NWAVE = number of wavelengths under consideration

CARD 5

Input Symbols

NN, GNU, CT
[FORMAT(I5,2D12.6)]

NN = number of Legendre coefficients

GNU = wavenumber (units cm^{-1})
CT = extinction coefficient (km^{-1})

CARD(S) 6

Input Symbols

OL(I)
[FORMAT D25.14]

OL(I) is the I^{th} Legendre expansion coefficient for the phase function.
NOTE: There should be NN cards of this type.

Subsequent Cards: NWAVE additional sets of type 5 and type 6 cards are required if NWAVE > 1.

PROGRAM LISTING

CLEM

```
      COMPILER (DIAG=3)
      IMPLICIT REAL*8(A-H,O-Z)
C     PROGRAM CLEM70 ..ADAPTED FROM CLEM65(26 MAR 1977 ) 12 OCT 1977
C     THIS VERSION CONCENTRATES ALL TEMP DATA IN A FEW CARDS.
C     ALSO INCLUDES H2O-VAPOR ABSORP. BELOW AND WITHIN THE CLOUD
C     WILL NOW LOOP ON WAVELENGTH - RCS
C     UNITS FOR ECLOUD AND ALL 'INTENSITIES' ARE  MILLI WATTS/
C     (SQ. METER-SR- INVERSE CENTIMETER)
C
    1 FORMAT(I5,3F10.6,I1)
    2 FORMAT(/' CONTINUUM ABSORPTION BY WATER-VAPOR WITHIN THE CLOUD YIE
     *LDS  K(VAPOR) = ',1PD12.5,'  PER KM.'/)
    3 FORMAT(/'  LAYER NO. ',I2,5X,'THICKNESS =',F9.5,5X,'TEMP = ',F7.3
     *,3X,'BNUC = ',1PD11.4,3X,'ECLOUD = ',D13.6/)
    4 FORMAT( ' WAVENUMBER = ',F 12.5,' CM -1.    SURFACE ALBEDO = ',
     *1PD13.6,'. CLOUD ALBEDO FOR SINGLE SCATTERING = ',D14.7/)
    5 FORMAT( ' SURFACE TEMP = ',F8.3,5X,'BNUS = ',1PD11.4,5X, 'ESURF =
     *',D13.6)
    6 FORMAT(/8(2X,1HL,4X,5HOMEGA,4X)/)
    7 FORMAT(8(1X,12,F13.9),4X)
    8 FORMAT(/'*** PHASE FUNCTION EXPANSION TRUNCATED TO 32 TERMS ***')
    9 FORMAT(1H ,'FOR A TOTAL DEPTH OF ',F8.3,'  KM  '/)
   10   FORMAT(1H1,' WAVENUMBER = ',G11.4,'   EXTINCTION COEFFICIENT = ',
     +G11.4,'  KM-1')
   11 FORMAT(  ///'   OTHER PARAMETERS  '/)
   12 FORMAT(/'  INTENSITIES FOR THE BASIC SLAB IF  ECLOUD = 1  '/)
   13 FORMAT('  ANGLE = ',F5.2,' DEG.',5X,' INTENS. = ',F9.5)
   17 FORMAT(' THE PHASE FUNCTION EXPANSION CONTAINED ',I3,' TERMS  ')
   18 FORMAT(10F8.2)
   19 FORMAT(D25.14)
   20 FORMAT(1H1,/)
   21 FORMAT(/)
  100 FORMAT (I5)
  101   FORMAT (I5,2D17.6)
C
      REAL TSS,TST,Y,Q3,ISNGL
      DIMENSION S(16,16,2),T(16,16,2),A(16,16),B(16,16),Q1(16,16)
      DIMENSION AS(16,16),BS(16,16),AT(16,16),BT(16,16),ALBUP(16)
      DIMENSION OL(32),EMU(16),SIG(16),W(16),ETS(16),EMO(16),Y(16)
      DIMENSION PL(16,16),P(16,16),R(16,16),Q(16,16),APT(16)
      DIMENSION G(16,16),ANG(16),Q2(16,16),EYUP(16),EYDN(16),TAUR(50)
      EQUIVALENCE(S(1),AS(1)),(S(257),BS(1))
      EQUIVALENCE(T(1),AT(1)),(T(257),BT(1))
      COMMON S,T,A,B,Q,Q1,P,R,PL,OL,EMU,EMO,W,ETS,SIG
      COMMON FM, TAUU,EMUO,TAUL, TAUI,TAUT,ALBUP  ,ECLOUD,MM,NN,L,LL
      COMMON NTI,NTF,KO
C     THIS STMT AND THE NEXT WILL NOT APPEAR IN FURTHER PGM LISTINGS
      CALL IO
      NCOUNT=0
      L=16
```

```
      PI=3.14159265358980+00
      FP=1.0D+00/(4.0D+00 *PI)
      CALL EMGUST
      DO 22 I=1,L
      EMU(I)=(1.00D+00-EMO(I))/2.0D+00
      W(I)=SIG(I)
      SIG(I)=1.0D+00/EMU(I)
      W(I)=W(I)*SIG(I)
   22 EMO(I)=180.0D+00*DACOS(EMU(I))/PI
      READ(05,1)NLYRS,THICK,ALBS,TMSC
      READ(05,1)MODEL,HEIGHT,PUNCH
      IPUNCH=0
      IF(PUNCH.LE.0.)IPUNCH=1
      READ(05,18)(TAUR(I),I=1,NLYRS)
      READ (05,100) NWAVE
  502 CONTINUE
      READ (5,101) NN,GNU,CT
      WRITE (6,10)  GNU,CT
      WRITE(6,17)NN
      IF(NN.LE.32)GO TO 23
      WRITE(6,8)
      NN=32
   23 DO 24 I=1,NN
   24 READ(05,19,END=241)OL(I)
  241 WRITE(6,6)
      WRITE(6,7)(I,OL(I),I=1,NN)
      WRITE(6,11)
C
      CALL VAPOR(HEIGHT,GNU,TAUA,MODEL)
      TMPS=TMSC+273.16D+00
      TAUI=THICK*CT
      ISNGL=(DLOG(TAUI)/(DLOG(2.D+00)))
      TST=20.0+ISNGL
      NTF=IFIX(TST)
      RNTF=NTF
      TST=TST-RNTF
      IF(TST.GE.0.10)NTF=NTF+1
      NTI=NTF
      CALL CLSTK(0,0)
      NTF=1
      ALBC=OL(1)
      IF(MODEL.NE.0)GO TO 245
      TMP=0.0
      GO TO 246
  245 TMP =TAUR(1)+273.16
      CALL VAPOR(HEIGHT,GNU,TMP,99)
  246 TAUI=TAUT
      TMPO=TMP
      TAUT= TAUI/(CT+TMP)
  100 DO 26 I=1,L
```

```
101             TA=0.D+00
102             DO 25 J=1,L
103          25 TA=TA+SIG(I)*W(J)*EMU(J)*P(I,J)*(1.D+00-ETS(J))/W(I)
104             Q1(I,1)=TA
105          24 OL(I)=TA
106             WRITE(6,9)GNU,ALBS,ALBC
107             CALL PLANCK(GNU,TMPS,BNUS)
108             FSURF=(1.D+00-ALBS)*BNUS
109             WRITE(6,5)TMSC,BNUS,FSURF
110       C
111             ILY=1
112             TMP=TAUR(1)+273.16D+00
113             CALL PLANCK(GNU,TMP,BNU)
114             ECLOUD=(1.D+00-ALBC )*BNU
115          27 WRITE(6,12)
116             DO 28 I=1,L
117             ANG(I)=5.D+00*DFLOAT(I-1)
118             EMUO=DCOS(ANG(I)*PI/180.D+00)
119             CALL EMNTRP(1)
120             WRITE(6,13)ANG(I),ALBUP(1)
121             Q1(I,5)=OL(I)*ECLOUD
122             ETS(I)=Q1(I,5)
123             Q1(1,6)= Q1(1,5)
124             DO 28 J=1,L
125             PL(I,J)=W(I)*EMU(J)*ALBS*FP*DEXP(-(TAUA*(SIG(I)+SIG(J))))
126             G(I,J)=A(I,J)
127             AT(I,J)=B(I,J)
128             BS(I,J)=A(I,J)
129             AS(I,J)=A(I,J)
130             RT(I,J)=B(I,J)
131          28 Q2(I,J)=B(I,J)
132             WRITE(6,20)
133             WRITE(6,3)NTF,TAUT ,TAUR(1),BNU,ECLOUD
134             WRITE(6,2)TMPO
135             CALL EMPR60(GNU,ESURF,FP,ALBS,TAUA,APT)
136       C     TAUL=TAUT
137       C     CALL DETECT (CT)
138             IF(IPUNCH.EQ.1)WRITE(4,40)MODEL,TAUT,APT(1),APT(4),APT(7),APT(10),
139            *APT(13)
140          40 FORMAT(1X,I1,6X,6(F9.3,3X))
141             IF(NLYRS.EQ.1)GO TO 33
142             IC=0
143       C
144          30 ILY=ILY+1
145             IF(ILY.GT.NLYRS)GO TO 33
146             IC=IC+1
147             IF(IC.EQ.2)WRITE(6,20)
148             IF(IC.EQ.1)WRITE(6,21)
149             IF(IC.EQ.2)IC=0
150             TMZC=TAUR(ILY)
```

```
151             TMP=TM7C+273.16D+00
152             CALL PLANCK(GNU,TMP,BNU)
153             ECLOUD=(1.D+00-ALBC)*BNU
154          31 CONTINUE
155             DO 32 I=1,L
156             QI(I,3)=OL(I)*ECLOUD
157             QI(I,4)=OL(I)*ECLOUD
158             QI(I,1)=QI(I,5)
159             QI(I,2)=QI(I,6)
160             IF(ILY.GT.2)ETS(I)=QI(I,11)
161             DO 32 J=1,L
162             A(I,J)=AS(I,J)
163             B(I,J)=AT(I,J)
164             P(I,J)=BS(I,J)
165             R(I,J)=BT(I,J)
166             AS(I,J)=G(I,J)
167             BS(I,J)=G(I,J)
168             AT(I,J)=Q2(I,J)
169          32 BT(I,J)=Q2(I,J)
170             TAUU=TAUT
171          &  IF(MODEL.NE.0)GO TO 325
172             TMP=0.0
173             GO TO 326
174         325 CONTINUE
175             CALL VAPOR (HEIGHT,GNU,TMP,99)
176         326 TAUL= TAUI/(CT+TMP)
177             WRITE(6,3)ILY,TAUL ,TM7C,BNU,ECLOUD
178             WRITE(6,2)TMP
179          C  ADDER COMBINES NEW LAYER WITH OLD RESULTANT LAYER
180             CALL ADDER(1)
181             WRITE(6,9)TAUT
182             CALL EMPR6D(GNU,ESURF,FP,ALBS,TAUA,APT)
183          C  CALL DETECT (CT)
184             IF(IPUNCH.EQ.1)WRITE(4,40)MODEL,TAUT,APT(1),APT(4),APT(7),APT(10),
185            *APT(13)
186             GO TO 30
187          33 NCOUNT=NCOUNT+1
188             IF ((NWAVE-NCOUNT).GT.0) GO TO 502
189             CALL EXIT
190             STOP
191             END
```

ADDER

```
      COMPILER (DIAG=3)
      SUBROUTINE ADDER (INHOMO)
      IMPLICIT REAL*8 (A-H,O-Z)
      DIMENSION S(16,16,2),T(16,16,2),A(16,16),B(16,16),QI(16,16)
      DIMENSION AS(16,16),BS(16,16),AT(16,16),BT(16,16),EYUPU(16)
      DIMENSION C(16,16),D(16,16),E(16,16),F(16,16),G(16,16),H(16,16)
      DIMENSION FLUXUP(16),FLUXDN(16),ALBUP(16),EYUPL(16),EYDNU(16)
      DIMENSION OL(32),EMU(16),SIG(16),W(16),ETS(16),EMO(16)
      DIMENSION PL(16,16),P(16,16),R(16,16),Q(16,16),EYDNL(16)
      EQUIVALENCE(S(1),AS(1)),(S(257),BS(1))
      EQUIVALENCE(T(1),AT(1)),(T(257),BT(1))
      COMMON S,T,A,B,Q,QI,P,R,PL,OL,EMU,EMO,W,ETS,SIG
      COMMON EM,  TAUU,EMUO,TAUL,TAUI,TAUT,ALBUP,  PHI,MM,NN,L,LL
      COMMON NTI,NTF,KO
C
      DO 1 I=1,L
      EYUPU(I)=QI(I,1)
      EYDNU(I)=QI(I,2)
      EYUPL(I)=QI(I,3)
      EYDNL(I)=QI(I,4)
      DO 2 J=1,L
      C(I,J)=P(I,J)
      D(I,J)=R(I,J)
      E(I,J)=AS(I,J)
      F(I,J)=AT(I,J)
      G(I,J)=BS(I,J)
      H(I,J)=BT(I,J)
      TAUT=TAUL+TAUU
C     DO 99 MM =1,NN
C     M=MM-1
      DO 3 J=1,L
      DO 3 I=1,L
      TA=0.0
      DO 2 K=1,L
    2 TA=TA-C(I,K)*E(K,J)
      IF(I.EQ.J)TA=TA+1.0
      QI(I,J)= TA
    3 Q(I,J)=TA
      CALL EMINV
      DO 5 J=1,L
      DO 5 I=1,L
      TA=0.0
      TB=0.0
      DO 4 K=1,L
    4 TA=TA+Q(I,K)*B(K,J)
      QI(I,J)=Q(I,J)
    5 R(I,J)=TA
      DO 7 J=1,L
      DO 7 I=1,L
      TA=0.0
```

```
      TB=0.0
      DO 6 K=1,L
      TA=TA+E(I,K)*P(K,J)
    6 TB=TB+E(I,K)*R(K,J)
      P(I,J)=TB
    7 AT(I,J)=TA
      DO 9 J=1,L
      DO 9 I=1,L
      TA=0.0
      DO 8 K=1,L
    8 TA=TA+D(I,K)*P(K,J)
    9 AS(I,J)=TA+A(I,J)
      IF(INHOMO.EQ.2)GO TO 11
      DO 10 I=1,L
      DO 10 J=1,L
      AS(I,J)=AS(I,J)
   10 AT(I,J)=AT(I,J)
      GO TO 20
   11 DO 13 J=1,L
      DO 13 I=1,L
      TA=0.0
      DO 12 K=1,L
   12 TA=TA-E(I,K)*C(K,J)
      IF(I.EQ.J)TA=TA+1.0
   13 Q(I,J)=TA
      CALL EMINV
      DO 15 J=1,L
      DO 15 I=1,L
      TA=0.0
      DO 14 K=1,L
   14 TA=TA+Q(I,K)*H(K,J)
   15 R(I,J)=TA
      DO 17 J=1,L
      DO 17 I=1,L
      TA=0.0
      TB=0.0
      DO 16 K=1,L
      TA=TA+D(I,K)*R(K,J)
   16 TB=TB+C(I,K)*R(K,J)
      AT(I,J)=TA
   17 R(I,J)=TB
      DO 19 J=1,L
      DO 19 I=1,L
      TA=0.0
      DO 18 K=1,L
   18 TA=TA+E(I,K)*P(K,J)
   19 AS(I,J)=G(I,J)+TA
   20 DO 22 I=1,L
      DO 22 J=1,L
      TA=0.0+00
```

```
101             TB=0.D+00
102             DO 21 K=1,L
103             TA=TA+F(I,K)*Q1(K,J)
104          21 TB=TB+F(I,K)*Q1(K,J)
105             A(I,J)=TA
106          22 B(I,J)=TB
107             DO 24 I=1,L
108             DO 24 J=1,L
109             TA=0.D+00
110             TB=0.D+00
111             DO 23 K=1,L
112             TA=TA+D(I,K)*A(K,J)
113          23 TB=TB+B(I,K)*C(K,J)
114             G(I,J)=TA
115          24 F(I,J)=TB
116             IF(INHOMO.EQ.0)GO TO 27
117             DO 26 I=1,L
118             DO 26 J=1,L
119             TA=0.D+00
120             DO 25 K=1,L
121          25 TA=TA+G(I,K)*C(K,J)
122          26 H(I,J)=TA+D(I,J)
123          27 DO 29 I=1,L
124             TA=0.D+00
125             FAI=SIG(I)/W(I)
126             DO 28 J=1,L
127          28 TA=TA+ (F(I,J)*EYUPL(J)+B(I,J)*EYDNU(J))*FAI*EMU(J)*W(J)
128             Q1(I,6)  =TA + EYDNL(I)
129          29 IF(INHOMO.EQ.0) Q1(I,5) =Q1(I,6)
130             IF(INHOMO.EQ.0)GO TO 32
131             DO 31 I=1,L
132             TA=0.D+00
133             FAI=SIG(I)/W(I)
134             DO 30 J=1,L
135          30 TA=TA+  (G(I,J)*EYDNU(J)+H(I,J)*EYUPL(J))*FAI *W(J)*EMU(J)
136          31 Q1(I,5)  =TA + EYUPU(I)
137          32 CONTINUE
138          33 CONTINUE
139             RETURN
140             END
```

CLSTK

```
      COMPILER (DIAG=3)
      SUBROUTINE  CLSTK(NEWOLD,IFAST)
      IMPLICIT REAL*8(A-H,O-Z)
      DIMENSION S(16,16,2),T(16,16,2),A(16,16),B(16,16),Q1(16,16)
      DIMENSION AS(16,16),BS(16,16),AT(16,16),BT(16,16),G(16,16)
      DIMENSION OL(32),EMU(16),SIG(16),W(16),ETS(16),EMO(16),ALBUP(16)
      DIMENSION PL(16,16),P(16,16),R(16,16),Q(16,16),PM(32,16)
      DIMENSION       C(16,16),F(16,16,2),FA(16,16),FB(16,16)
      EQUIVALENCE(S(1),AS(1)),(S(257),BS(1))
      EQUIVALENCE (F(1),FA(1)),(F(257),FB(1))
      EQUIVALENCE(T(1),AT(1)),(T(257),BT(1))
      COMMON S,T,A,B,Q,Q1,P,R,PL,OL,EMU,EMO,W,ETS,SIG
      COMMON EM    ,TAU,EMUO,TAUL,TAUI,TAUT,ALBUP   ,PHI,MM,NN,L,LL
      COMMON NTI,NTF,KO
      DO 1 J=1,L
      PM(1,J)=1.0D+00
    1 PM(2,J)=EMU(J)
      DO 2 I=3,NN
      FI=I-1
      DO 2 J=1,L
    2 PM(I,J)=((2.0*FI-1.0)*EMU(J)*PM(I-1,J)-(FI-1.0)*PM(I-2,J))/FI
      GAMMA=-1.0D+00
      MM=1
      M=0
      IF(NEWOLD.NE.0)GO TO 7
      GAMMA=-GAMMA
      EM=M
      EPS=1.0D+00
    3 FORE=1.0/(4.0*EPS)
      TAU=TAUI*2.0**(-NTI)
      DO 4 I=1,L
    4 ETS(I)=DEXP(-TAU*SIG(I))
      DO 6 J=1,L
      DO 6 I=1,L
      F(J,I,1)=0.0D+00
      IF(I.EQ.J)F(J,I,1)=1.0D+00
      P(I,J)=0.0D+00
      R(I,J)=0.0D+00
      GAM=-1.0D+00
      DO 5 LL=MM,NN
      GAM=-GAM
      P(I,J)=OL(LL)*PM(LL,J)*PM(LL,I)+P(I,J)
    5 R(I,J)=OL(LL)*PM(LL,J)*PM(LL,I)*GAM+R(I,J)
      TEMP=TAU*(1.0-0.5*TAU*(SIG(I)+SIG(J)))*FORE*EPS
      S(I,J,1)=TEMP*R(I,J)*W(I)
      T(I,J,1)=TEMP*P(I,J)*W(I)
      IF(I.EQ.J)T(I,J,1)=T(I,J,1)+ETS(I)
    6 CONTINUE
      GO TO 9
    7 TAUI=TAUT
```

```
      DO 8 I=1,L
      DO 8 J=1,L
      AS(I,J)=A(I,J)
      AT(I,J)=B(I,J)
    8 FA(I,J)=P(I,J)
      NTI=0
    9 LA=2
      LB=1
      DO 26 IT=1,NTF
      IP=IT-NTI
      KO=LA
      LA=LB
      LB=KO
      QK=0.0D+00
      DO 11 J=1,L
      DO 11 I=1,L
      TA=0.0D+00
      DO 10 K=1,L
   10 TA=TA-S(I,K,LA)*S(K,J,LA)
      IF(I.EQ.J)TA=TA+1.0D+00
      IF(I.NE.J.AND.DABS(TA).GE.QK)QK=DABS(TA)
   11 Q(I,J)=TA
      IF(QK.LE.1.0E-03.AND.IFAST.NE.0)GO TO 12
      CALL EMINV
      GO TO 14
   12 DO 13 I=1,L
      DO 13 J=1,L
      Q(I,J)=-Q(I,J)
      IF(I.EQ.J)Q(I,J)=2.0+Q(I,J)
   13 CONTINUE
   14 DO 16 J=1,L
      DO 16 I=1,L
      TA=0.0D+00
      TB=0.0D+00
      DO 15 K=1,L
      TA=TA+Q(I,K)*T(K,J,LA)
   15 TB=TB+T(I,K,LA)*S(K,J,LA)
      A(I,J)=TA
   16 B(I,J)=TB
      DO 18 J=1,L
      DO 18 I=1,L
      TA=0.0D+00
      TB=0.0D+00
      DO 17 K=1,L
      TA=TA+T(I,K,LA)*A(K,J)
   17 TB=TB+B(I,K)*A(K,J)
      T(I,J,LB)=TA
   18 S(I,J,LB)=S(I,J,LA)+TB
      DO 19 I=1,L
      DO 19 J=1,L
```

```
101             TA=0.0D+00
102             TA=S(I,J,LA)
103             IF(I.EQ.J)TA=TA+1.0D+00
104          19 C(I,J)=TA
105             DO 21 I=1,L
106             DO 21 J=1,L
107             TA=0.0D+00
108             DO 20 K=1,L
109          20 TA=TA+Q(I,K)*C(K,J)
110          21 Q1(I,J)=TA
111             DO 23 I=1,L
112             DO 23 J=1,L
113             TA=0.0D+00
114             DO 22 K=1,L
115          22 TA=TA+T(I,K,LA)*Q1(K,J)
116             IF(I.EQ.J)TA=TA+1.0D+00
117          23 G(I,J)=TA
118             DO 25 I=1,L
119             DO 25 J=1,L
120             TA=0.0D+00
121             DO 24 K=1,L
122          24 TA=TA+G(I,K)*F(K,J,LA)
123          25 F(I,J,IB)=TA
124          26 TAU=TAU*2.0**IP
125             GO TO(27,29),IB
126          27 TAUT=TAU
127             DO 28 I=1,L
128             DO 28 J=1,L
129             A(I,J)=AS(I,J)
130             B(I,J)=AT(I,J)
131          28 P(I,J)=FA(I,J)
132             GO TO 31
133          29 TAUT=TAU
134             DO 30 I=1,L
135             DO 30 J=1,L
136             A(I,J)=BS(I,J)
137             B(I,J)=BT(I,J)
138          30 P(I,J)=FB(I,J)
139          31 RETURN
140             END
```

EMGUST

```
      COMPILER (DIAG=3)
      SUBROUTINE EMGUST
      IMPLICIT REAL*8(A-H,O-Z)
      DIMENSION S(16,16,2),T(16,16,2),A(16,16),B(16,16),QI(16,16)
      DIMENSION AS(16,16),BS(16,16),AT(16,16),BT(16,16),Z(16)
      DIMENSION OL(32),EMU(16),SIG(16),W(16),ETS(16),EMO(16)
      DIMENSION PL(16,16),P(16,16),R(16,16),Q(16,16),PA(17),ALBUP(16)
      EQUIVALENCE(S(1),AS(1)),(S(257),BS(1))
      EQUIVALENCE(T(1),AT(1)),(T(257),BT(1))
      COMMON S,T,A,B,Q,QI,P,R,PL,OL,EMU,EMO,W,ETS,SIG
      COMMON EM    ,TAU,EMUO,TAUL,TAUI,TAUT,ALBUP   ,PHI,MM,NN,L,LL
      COMMON NTI,NTF,KO
      TOL=1.0D-14
      N=L
      PI=3.1415926535898D+00
      AA=2.0D+00/PI**2.0D+00
      AB=-62.D+00/(3.D+00*PI**4.D+00)
      AC=15116.D+00/(15.D+00*PI**6.D+00)
      AD=-12554474.D+00/(105.D+00*PI**8.D+00)
      PA(1)=1.000D+00
      EN=N
      NPI=N+1
      U=1.000D+00-(2.000D+00/PI)**2.D+00
      D= 1.0D+00/DSQRT((EN+0.5D+00)**2+U/4.0D+00)
      DO 7 I=1,N
      SM=I
      AZ=4.D+00*SM-1.D+00
      AE=AA/AZ
      AF=AB/AZ**3.D+00
      AG=AC/AZ**5.D+00
      AH=AD/AZ**7.D+00
    1 Z(I)=0.25D+00*PI*(AZ+AE+AF+AG+AH)
      DO 6 K=1,N
      X=DCOS(Z(K)*D)
    2 PA(2)=X
      DO 3 NN=3,NPI
      ENN=NN-1
    3 PA(NN)=((2.0D+00*ENN-1.000D+00)*X*PA(NN-1)-(ENN-1.0D+00)*PA(NN-2))/
     *FNN
      PNP=EN*(PA(N)-X*PA(NPI))/(1.0D+00-X*X)
      XI=X-PA(NPI)/PNP
      XD=DABS(XI-X)
      XDD=XD-TOL
      IF(XDD)5,5,4
    4 X=XI
      GO TO 2
    5 EMO(K)=X
      XF=DABS(EN*PA(N))
    6 SIG(K)=      2.0D+00*(1.0D+00-X*X)/(   XF     ) **2.0D+00
      RETURN
```

```
      EMGUST

      END
```

EMINV

```
      COMPILER (DIAG=3)
      SUBROUTINE EMINV
      IMPLICIT REAL*8(A-H,O-Z)
      DIMENSION S(16,16,2),T(16,16,2),A(16,16),B(16,16),QM(256)
      DIMENSION AS(16,16),BS(16,16),AT(16,16),BT(16,16),Q1(16,16)
      DIMENSION OL(32),EMU(16),SIG(16),W(16),ETS(16),EMO(16),ALBUP(16)
      DIMENSION PL(16,16),P(16,16),R(16,16),Q(16,16),JC(16),JCI(16)
      EQUIVALENCE(S(1),AS(1)),(S(257),BS(1))
      EQUIVALENCE(QM(1),Q(1))
      EQUIVALENCE(T(1),AT(1)),(T(257),BT(1))
      COMMON S,T,A,B,Q,Q1,P,R,PL,OL,EMU,EMO,W,ETS,SIG
      COMMON EM    ,TAU,EMUO,TAUL,TAUI,TAUT,ALBUP   ,PHI,MM,MN,L,LL
      COMMON NTI,NTF,KO
      N=L
      D=1.0D+00
      NK=-N
      DO 79 K=1,N
      NK=NK+N
      JC(K)=K
      JCI(K)=K
      KK=NK+K
      BIGA=QM(KK)
      DO 3 J=K,N
      IZ=N*(J-1)
      DO 3 I=K,N
      IJ=IZ+I
    1 IF(DABS(BIGA)-DABS(QM(IJ))) 2,3,3
    2 BIGA=QM(IJ)
      JC(K)=I
      JCI(K)=J
    3 CONTINUE
      J=JC(K)
      IF(J-K) 6,6,4
    4 KI=K-N
      DO 5 I=1,N
      KI=KI+N
      HOLD=-QM(KI)
      JI=KI-K+J
      QM(KI)=QM(JI)
    5 QM(JI)=HOLD
    6 I=JCI(K)
      IF(I-K) 9,9,7
    7 JP=N*(I-1)
      DO 8 J=1,N
      JK=NK+J
      JI=JP+J
      HOLD=-QM(JK)
      QM(JK)=QM(JI)
    8 QM(JI)=HOLD
    9 IF(BIGA) 11,10,11
```

```
      10 D=0.0D+00
         RETURN
      11 DO 13 I=1,N
         IF(I-K) 12,13,12
      12 IK=NK+I
         QM(IK)=QM(IK)/(-BIGA)
      13 CONTINUE
         DO 16 I=1,N
         IK=NK+I
         HOLD=QM(IK)
         IJ=I-N
         DO 16 J=1,N
         IJ=IJ+N
         IF(I-K) 14,16,14
      14 IF(J-K) 15,16,15
      15 KJ=IJ-I+K
         QM(IJ)=HOLD*QM(KJ)+QM(IJ)
      16 CONTINUE
         KJ=K-N
         DO 18 J=1,N
         KJ=KJ+N
         IF(J-K) 17,18,17
      17 QM(KJ)=QM(KJ)/BIGA
      18 CONTINUE
         D=D*BIGA
         QM(KK)=1.0D+00/BIGA
      19 CONTINUE
         K=N
      20 K=(K-1)
         IF(K) 27,27,21
      21 I=JC(K)
         IF(I-K)24,24,22
      22 JQ=N*(K-1)
         JR=N*(I-1)
         DO 23 J=1,N
         JK=JQ+J
         HOLD=QM(JK)
         JI=JR+J
         QM(JK)=-QM(JI)
      23 QM(JI)=HOLD
      24 J=JC(K)
         IF(J-K) 20,20,25
      25 KI=K-N
         DO 26 I=1,N
         KI=KI+N
         HOLD=QM(KI)
         JI=KI-K+J
         QM(KI)=-QM(JI)
      26 QM(JI)= HOLD
         GO TO 20
```

```
101          27 RETURN
102             END
```

FMNTRP

```
      COMPILER (DIAG=3)
      SUBROUTINE FMNTRP(NV)
      IMPLICIT REAL*8(A-H,O-Z)
      DIMENSION S(16,16,2),T(16,16,2),A(16,16),B(16,16),QI(16,16)
      DIMENSION AS(16,16),BS(16,16),AT(16,16),BT(16,16),ALBUP(16)
      DIMENSION OL(32),EMU(16),SIG(16),W(16),ETS(16),EMO(16),ELX(4)
      DIMENSION PL(16,16),P(16,16),R(16,16),Q(16,16)
      EQUIVALENCE(S(1),AS(1)),(S(257),BS(1))
      EQUIVALENCE(T(1),AT(1)),(T(257),BT(1))
      COMMON S,T,A,B,Q,QI,P,R,PL,OL,EMU,EMO,W,ETS,SIG
      COMMON FM    ,TAU,EMUO,TAUL,TAUT,TAUT,ALBUP   ,PHI,MM,NN,L,LL
      COMMON NTI,NTF,KO
      DO 1 I=1,L
      IF(EMUO.LE.EMU(I)) GO TO 2
    1 CONTINUE
      GO TO 4
    2 IF(I.EQ.1) GO TO 3
      IF(I.EQ.2) GO TO 3
      IF(I.EQ.L ) GO TO 4
      IMN=I-2
      IMX=I+1
      GO TO 5
    3 IMN=1
      IMX=4
      GO TO 5
    4 IMN=L -3
      IMX=L
    5 DO 6 I=1,4
    6 ELX(I)=1.D0+00
      DO 7 I=IMN,IMX
      IP=I+1-IMN
      DO 7 J=IMN,IMX
      IF(I.NE.J)ELX(IP)=ELX(IP)*(EMUO-EMU(J))/(EMU(I)-EMU(J))
    7 CONTINUE
      DO 8 J=1,NV
      ALBUP(J)=0.(D+00
      DO 8 I=IMN,IMX
      IP=I+1-IMN
    8 ALBUP(J)=ALBUP(J)+ELX(IP)*QI(I,J)
      RETURN
      END
```

```
1             COMPILER (DIAG=3)
2             SUBROUTINE EMPR60(GNU,FSURF,FP,ALBS,TAUA,APT)
3             IMPLICIT REAL*8(A-H,O-Z)
4           1 FORMAT(/1X,5HANGLE,6X,10HCLOUD I-DN,6X,10HCLOUD I-UP,  4X,12HSURFA
5            *CE I-UP,2X,12HSURFACE I-DN,4X,10HTOTAL I-DN,7X,10HTOTAL I-UP,  2X,
6            *13HAPPARENT TEMP,2X,12HTRANSMISSION/)
7           2 FORMAT(1X,F5.2,8(6X,F9.4))
8       C
9       C       19 APRIL 1976   'SECOND VERSION'
10            REAL TSS,TST,Y,Q3
11            DIMENSION S(16,16,2),T(16,16,2),A(16,16),B(16,16),Q1(16,16)
12            DIMENSION AS(16,16),BS(16,16),AT(16,16),BT(16,16),ALBUP(16)
13            DIMENSION QL(32),EMU(16),SIG(16),W(16),ETS(16),EMO(16),Y(16)
14            DIMENSION PL(16,16),P(16,16),R(16,16),Q(16,16),APT(16)
15            DIMENSION G(16,16),          Q2(16,16),EYUP(16),EYDN(16),TAUR(50)
16            EQUIVALENCE(S(1),AS(1)),(S(257),BS(1))
17            EQUIVALENCE(T(1),AT(1)),(T(257),BT(1))
18            COMMON S,T,A,B,Q,Q1,P,R,PL,QL,EMU,EMO,W,ETS,SIG
19            COMMON EM, TAUU,EMUO,TAUL, TAUI,TAUT,ALBUP  ,PHI,MM,NN,L,LL
20            COMMON NTI,NTF,KO
21            DO 3 I=1,L
22          3 EYUP(I)=SIG(I)*EMU(I)*FSURF*DEXP(-TAUA*SIG(I))
23            IF(ALBS.EQ.0.D+00)GO TO 10
24            DO 5 I=1,L
25            DO 5 J=1,L
26            TA = 0.D+00
27            DO 4 K=1,L
28          4 TA=TA-PL(I,K)*BS(K,J)
29            IF(I.EQ.J)TA=1.D+00+TA
30          5 Q(I,J)=TA
31            CALL EMINV
32            DO 7 I=1,L
33            DO 7 J=1,L
34            TA=0.D+00
35            TB=0.D+00
36            DO 6 K=1,L
37            TA=TA+BT(I,K)*Q(K,J)
38          6 TB=TB+BS(I,K)*Q(K,J)
39            R(I,J)=TA
40          7 P(I,J)=TB
41            DO 9 I=1,L
42            DO 9 J=1,L
43            TA = 0.D+00
44            DO 8 K=1,L
45          8 TA=TA+R(I,K)*PL(K,J)
46          9 R(I,J)=TA
47         10 IF(ALBS.NE.1.D+00)GO TO 12
48            DO 11 I=1,L
49            DO 11 J=1,L
50            P(I,J)=BS(I,J)
```

```
51              R(I,J)=RT(I,J)
52              R(I,J)=0.D+00
53           11 PL(I,J)=0.D+00
54           12 DO 14 I=1,L
55              TA=0.D+00
56              TB=0.D+00
57              DO 13 J=1,L
58              FA=SIG(I)*W(J)*EMU(J)/W(I)
59              TA=TA+FA*B(I,J)*FYUP(J)
60           13 TB = TB + FA*R(I,J)*QI(J,5)
61              QI(I,7)=TA
62           14 QI(I,11)=TB+QI(I,6)
63              DO 16 I=1,L
64              DO 15 J=1,L
65              TA=0.D+00
66              DO 15 K=1,L
67           15 TA=TA+ R(I,J)*PL(K,J)
68           16 R(I,J)=TA
69              DO 18 I=1,L
70              TA=0.D+00
71              TB=0.D+00
72              DO 17 J=1,L
73              FA=SIG(I)*W(J)*EMU(J)/W(I)
74              TA=TA+FA*P(I,J)*FYUP(J)
75           17 TB=TB+FA*R(I,J)*QI(J,5)
76              QI(I,10)=TA
77              QI(I,8) =TB+QI(I,5)
78              QI(I,9)=QI(I,8)+QI(I,10)
79              QI(I,16)=(QI(I,11)-(PHI*QL(I)))/ETS(I)
80              ETS(I)=QI(I,11)
81           18 QI(I,12)=QI(I,7) +QI(I,11)
82              DO 19 I=1,L
83              QI(I,13)=QI(I,7)/ESURF
84           19 QI(I,14)=((1.44D+00*GNU)/(DLOG(1.D+00+((1.1934D-05*GNU**3.D+00)
85             */(QP(I,12))))))-273.16D+00
86              WRITE(4,1)
87              RADS=1.D+00/(FP*7.2D+02)
88              DO 20 I=1,16
89              ANG =5.00+0)*DFLOAT(I-1)
90              EMU0=DCOS(ANG*RADS)
91              CALL EMNTRP(16)
92              APT(I)=ALBUP(14)
93           20 WRITE(4,2)ANG,ALBUP(8),ALBUP(11),ALBUP(7),ALBUP(10),ALBUP(9),
94             *ALBUP(12),ALBUP(14),ALBUP(16)
95              RETURN
96              END
```

```
      SUBROUTINE IO
      DIMENSION DUMMY(20)
      PRINT 100
  100 FORMAT (1H1,'*** THE FOLLOWING IS THE PROPER INPUT DATA',
     +' TO GO WITH THE SUBSEQUENT OUTPUT',/)
      DO 1 I=1,38
      READ (5,101,END=2) (DUMMY(J),J=1,20)
      WRITE (6,101) (DUMMY(K),K=1,20)
    1 CONTINUE
    2 CONTINUE
      PRINT 102
  102 FORMAT (1H2,' *** END INPUT')
  101 FORMAT (20A4)
      RETURN
      END
```

PLANCK

```
1               COMPILER (DIAG=3)
2               SUBROUTINE PLANCK(GNU,TMP,BNU)
3               DOUBLE PRECISION BNU,TMP,GNU,DEXP
4               IF(TMP.LT.5.D+01)GO TO 1
5               BNU=1.1934D-05*(GNU**3.D+00)/(DEXP(1.44D+00*GNU/TMP)-1.D+00)
6               GO TO 2
7             1 BNU=0.D+00
8             2 RETURN
9               END
```

VAPOR

```
      COMPILER (DIAG=3)
      SUBROUTINE VAPOR(HT,GNUD,TAU,MODEL)
      DOUBLE PRECISION TAU, GNUD,HT
C     FOR CALCULATING OPTICAL DEPTH (TAUA) OF WATER-VAPOR (DUE TO
C     CONTINUUM ABSORPTION IN THE 500 TO 1250 CM-1 RANGE) BETWEEN THE
C     BASE OF A CLOUD (HEIGHT=DISTANCE IN KM BETWEEN BASE AND SURFACE)
C     AND THE SURFACE.
C       MODEL 1 IS THE AFCRL TROPICAL ATMOSPHERIC MODEL
C       MODEL 2 IS THE AFCRL MIDLATITUDE SUMMER MODEL
C       MODEL 3 IS THE AFCRL MIDLATITUDE WINTER MODEL
C       MODEL 4 IS THE 1962 US STANDARD ATMOSPHERE MODEL
C     ** SEE SELBY,ROBERTS + BIBERMAN (1976) FOR ABSORP. MODEL **
C
C       MODEL=99 ASSUMES SATURATION AT TEMP='TAU'
      DIMENSION Z(10),WR(10),TR(10),WRH(10,4),TRH(10,4)
      DATA Z/0.,1.,2.,3.,4.,5.,6.,7.,8.,9./
      DATA WRH/19.,13.,9.3,4.7,2.2,1.5,.85,.47,.25,.12,
     .         14.,9.3,5.9,3.3,1.9,1.,.61,.37,.21,.12,
     .         3.5,2.5,1.8,1.2,.66,.38,.21,.085,.035,.016,
     .         5.9,4.2,2.9,1.8,1.1,.64,.38,.21,.12,.046/
      DATA TRH/300.,294.,288.,284.,277.,270.,264.,257.,250.,244.,
     .         294.,293.,285.,279.,273.,267.,261.,255.,248.,242.,
     .       272.2,268.7,265.2,261.7,255.7,249.7,243.7,237.7,231.7,225.7,
     .       288.1,281.6,275.1,268.7,262.2,255.7,249.2,242.7,236.2,229.7/
    1 FORMAT(/'  **** THE VALUE GNU = ',E10.6,' IS OUTSIDE THE DATA RANG
     .E FOR CONTINUUM ABSORPTION DATA.  TAUA SET = 0.0 **'/)
    8 FORMAT(/' *** CLOUD-BASE HEIGHT OF ',E12.5,' KM. EXCEEDS INTERNAL
     .DATA RANGE ...HEIGHT REDUCED TO 9.0 KM **'/)
    2 FORMAT(/1X,' ATMOSPHERIC MODEL FOR SUB-CLOUD ABSORPTION = ',I2,'.
     .OPTICAL DEPTH ( TAUA ) = ',E12.5,'  CLOUD BASE HEIGHT = ',E12.5,'
     . KM'/)
    7 FORMAT(/' ***   MODEL NO. ',I3,'  IS UNDEFINED. TAUA SET TO ZERO'/
     .)
      GNU=SNGL(GNUD)
      IF(GNU.LT.500.0.OR.GNU.GT.1250.)GO TO 3
      GO TO 4
    3 WRITE(6,1)GNU
      GO TO 6
    4 HEIGHT=SNGL(HT)
      IF(HEIGHT.LE.9.)GO TO 5
      WRITE(6,8)HEIGHT
      HEIGHT=9.0
    5 CSO=1.25E-22*(1.+1336.*EXP(-7.87E-3*GNU))
      CAYC=0.0
      IF(MODEL.EQ.99)GO TO 70
      IF (MODEL.GE.1.AND.MODEL.LE.4)GO TO 9
    6 CAYC=0.0
      IF(MODEL.EQ.0)GO TO 99
      WRITE(6,7)MODEL
      GO TO 99
```

```
      9 DO 10 I=1,10
        WR(I)=WRH(I,MODEL)
     10 TR(I)=TRH(I,MODEL)
        NMX=1 + IFIX(HEIGHT)
        ILAST=IFIX((HEIGHT-FLOAT(NMX-1))*10.)
        IF((HEIGHT-(FLOAT(NMX-1)+.1*FLOAT(ILAST))).GE.0.05)ILAST=ILAST+1
        IMX=10
        CAYC=0.0
        DO 60 N=1,NMX
        IF(N.EQ.NMX)IMX=ILAST
        IF(IMX.EQ.0)GO TO  99
        DZ=Z(N+1)-Z(N)
        A1=(WR(N)*Z(N+1)-WR(N+1)*Z(N))/DZ
        A2=(WR(N+1)-WR(N))/DZ
        B1=(TR(N)*Z(N+1)-TR(N+1)*Z(N))/DZ
        B2=(TR(N+1)-TR(N))/DZ
        DO 55 I=1,IMX
        ZC=FLOAT(N-1)+((.1*FLOAT(I))-.05)
        W=A1+A2*ZC
        T=B1+B2*ZC
        PW=4.54E-5*T*W **1
        WH2O=W*3.34E16
        FACT=CSO*PW*WH2O*EXP(1800.*((1./T) -.00337B)) * 1.E5
        CAYC=CAYC+FACT
     55 CONTINUE
     60 CONTINUE
     99 TAUA=CAYC*.1
        WRITE(6,2)MODEL,TAUA,HEIGHT
        TAU=DBLE(TAUA)
        GO TO 100
     70 T=SNGL(TAU)
        ES=6.108 *EXP(5.453E+3*(3.663E-3-(1./T)))
        W=216.5*ES/T
        PW=4.54E-5*T*W **1
        WH2O=W*3.34E16
        CAYC=CSO*PW*WH2O*EXP(1800.*((1./T) -.00337B)) * 1.E5
        TAU=DBLE(CAYC)
    100 RETURN
        END
```

SAMPLE INPUT DATA

```
*** THE FOLLOWING IS THE PROPER INPUT DATA TO GO WITH THE SUBSEQUENT OUTPUT

  20  0.100000  0.000000 30.000000
   1  2.0      +00.00001
-0.2500 -0.7500 -1.2500 -1.7500 -2.2500 -2.7500 -3.2500 -3.7500 -4.2500 -4.7500
-5.2500 -5.7500 -6.2500 -6.7500 -7.2500 -7.7500 -8.2500 -8.7500 -9.2500 -9.7500
   1
  32 .100000+004 .115078+003
     .670789037235256+000    0
     .188149983241l4+001     1
     .285754761607el+001     2
     .357901994037l9+001     3
     .406801354733el+001     4
     .435562352344l7+001     5
     .447165220424l5+001     6
     .444433646209l0+001     7
     .429876215376l5+001     8
     .406082465608l6+001     9
     .375145998041l1+001    10
     .339457048826l7+001    11
     .300737923066l5+001    12
     .260984279762l4+001    13
     .221492959112l3+001    14
     .183692630027l6+001    15
     .148409657362l1+001    16
     .116473505607l1+001    17
     .883047487759l9+000    18
     .641847823555l9+000    19
     .442866468720l4+000    20
     .284706530166l9+000    21
     .167274324408l4+000    22
     .872981129864l2-001    23
     .404402993575l6-001    24
     .161546288503l4-001    25
     .573681868616l2-002    26
     .179324245331l2-002    27
     .499369603771l5-003    28
     .125082179198l3-003    29
     .284174254l692-004     30
     .572822997639l6-005    31
*** END INPUT
```

WAVENUMBER = .1000+004 EXTINCTION COEFFICIENT = .1151+003 KM-1
THE PHASE FUNCTION EXPANSION CONTAINED 32 TERMS

L	OMEGA	L	OMEGA	L	OMEGA	L	OMEGA	L	OMEGA	L	OMEGA	L	OMEGA	L	OMEGA
1	.670789037	2	1.881499832	3	2.857547616	4	3.579019940	5	4.068013547	6	4.355623523	7	4.471652204	8	4.444336462
9	4.298762154	10	4.060824656	11	3.751459980	12	3.394570488	13	3.007379231	14	2.609842798	15	2.214929591	16	1.836926300
17	1.484096574	18	1.164735056	19	.883047488	20	.641847824	21	.442866469	22	.284706530	23	.167274324	24	.087298113
25	.040440299	26	.016154629	27	.005736819	28	.001793242	29	.000499370	30	.000125082	31	.000028417	32	.000005728

OTHER PARAMETERS

ATMOSPHERIC MODEL FOR SUB-CLOUD ABSORPTION = 1. OPTICAL DEPTH (TAUA) = .33163+00 CLOUD BASE HEIGHT = .20000+01 KM

WAVENUMBER = 1000.00000 CM -1. SURFACE ALBEDO = 0.000000 . CLOUD ALBEDO FOR SINGLE SCATTERING = 6.7078904-001

SURFACE TEMP = 30.000 BNUS = 1.0415+002 FSURF = 1.041539+002

INTENSITIES FOR THE BASIC SLAB IF ECLOUD = 1

ANGLE =	.00 DEG.	INTENS. =	2.99043
ANGLE =	5.00 DEG.	INTENS. =	2.99073
ANGLE =	10.00 DEG.	INTENS. =	2.99159
ANGLE =	15.00 DEG.	INTENS. =	2.99286
ANGLE =	20.00 DEG.	INTENS. =	2.99434
ANGLE =	25.00 DEG.	INTENS. =	2.99573
ANGLE =	30.00 DEG.	INTENS. =	2.99667
ANGLE =	35.00 DEG.	INTENS. =	2.99673
ANGLE =	40.00 DEG.	INTENS. =	2.99541
ANGLE =	45.00 DEG.	INTENS. =	2.99207
ANGLE =	50.00 DEG.	INTENS. =	2.98584
ANGLE =	55.00 DEG.	INTENS. =	2.97552
ANGLE =	60.00 DEG.	INTENS. =	2.95912
ANGLE =	65.00 DEG.	INTENS. =	2.93315
ANGLE =	70.00 DEG.	INTENS. =	2.89135
ANGLE =	75.00 DEG.	INTENS. =	2.82130

LAYER NO. 1 THICKNESS = .09997 TEMP = -.250 BNUC = 6.1302+001 ECLOUD = 2.018115+001

CONTINUUM ABSORPTION BY WATER-VAPOR WITHIN THE CLOUD YIELDS K(VAPOR) = 3.04375-002 PER KM.

ANGLE	CLOUD I-DN	CLOUD I-UP	SURFACE I-UP	SURFACE I-DN	TOTAL I-DN	TOTAL I-UP	APPARENT TEMP	TRANSMISSION
.00	60.3503	60.3503	.7208	.2778	60.6281	61.0711	-.4437	.0000
5.00	60.3564	60.3564	.7103	.2800	60.6364	61.0867	-.4474	.0000
10.00	60.3736	60.3736	.6797	.2871	60.6607	61.0533	-.4586	.0000
15.00	60.3994	60.3994	.6315	.2993	60.6987	61.0309	-.4775	.0000
20.00	60.4293	60.4293	.5696	.3176	60.7469	60.9969	-.5045	.0000
25.00	60.4574	60.4574	.4963	.3434	60.8007	60.9562	-.5404	.0000
30.00	60.4763	60.4763	.4243	.3785	60.8549	60.9007	-.5872	.0000
35.00	60.4775	60.4775	.3510	.4260	60.9036	60.8285	-.6481	.0000
40.00	60.4508	60.4508	.2827	.4900	60.9409	60.7335	-.7283	.0000
45.00	60.3834	60.3834	.2223	.5767	60.9601	60.6056	-.8363	.0000
50.00	60.2576	60.2576	.1712	.6953	60.9529	60.4288	-.9859	.0000
55.00	60.0495	60.0495	.1295	.8583	60.9079	60.1790	-1.1977	.0000
60.00	59.7184	59.7184	.0967	1.0862	60.8045	59.8150	-1.5074	.0000
65.00	59.1943	59.1943	.0714	1.4083	60.6025	59.2057	-1.9768	.0000
70.00	58.3508	58.3508	.0524	1.8683	60.2191	58.4052	-2.7194	.0000
75.00	56.9370	56.9370	.0382	2.5271	59.4641	56.9752	-3.9641	.0000

LAYER NO. 2 THICKNESS = .09998 TEMP = -.750 BNUC = 6.0708+001 ECLOUD = 1.998565+001

CONTINUUM ABSORPTION BY WATER-VAPOR WITHIN THE CLOUD YIELDS K(VAPOR) = 2.86819-002 PER KM.

FOR A TOTAL DEPTH OF .200 KM

ANGLE	CLOUD I-DN	CLOUD I-UP	SURFACE I-UP	SURFACE I-DN	TOTAL I-DN	TOTAL I-UP	APPARENT TEMP	TRANSMISSION
.00	60.9765	60.3979	.0047	.2778	61.2542	60.4026	-1.0082	.0105
5.00	60.9737	60.3950	.0046	.2801	61.2538	60.3996	-1.0107	.0103
10.00	60.9653	60.3861	.0044	.2871	61.2524	60.3905	-1.0184	.0099
15.00	60.9504	60.3706	.0040	.2993	61.2497	60.3746	-1.0318	.0092
20.00	60.9278	60.3472	.0036	.3177	61.2455	60.3508	-1.0520	.0083
25.00	60.8955	60.3141	.0031	.3434	61.2389	60.3171	-1.0806	.0073
30.00	60.8504	60.2681	.0026	.3786	61.2289	60.2707	-1.1199	.0062
35.00	60.7880	60.2051	.0021	.4261	61.2140	60.2072	-1.1739	.0052
40.00	60.7016	60.1184	.0017	.4900	61.1917	60.1201	-1.2478	.0042
45.00	60.5810	59.9980	.0013	.5767	61.1578	59.9993	-1.3506	.0033
50.00	60.4101	59.8278	.0010	.6953	61.1053	59.8286	-1.4957	.0026
55.00	60.1649	59.5843	.0008	.8583	61.0233	59.5851	-1.7037	.0019
60.00	59.8045	59.2269	.0006	1.0862	60.8907	59.2274	-2.0098	.0015
65.00	59.2579	58.6851	.0004	1.4083	60.6662	58.6855	-2.4758	.0011
70.00	58.3975	57.8327	.0003	1.8683	60.2658	57.8330	-3.2144	.0008
75.00	56.9710	56.4198	.0002	2.5271	59.4981	56.4200	-4.4536	.0006

LAYER NO. 19 THICKNESS = .09999 TEMP = -9.250 BNDC = 5.1163+001 ECLOUD = 1.0643+001

CONTINUUM ABSORPTION BY WATER-VAPOR WITHIN THE CLOUD YIELDS K(VAPOR) = 1.0067-002 PER KM.

FOR A TOTAL DEPTH OF 1.900 KM

ANGLE	CLOUD I-DN	CLOUD I-UP	SURFACE I-UP	SURFACE I-DN	TOTAL I-DN	TOTAL I-UP	APPARENT TEMP	TRANSMISSION
.00	60.9806	50.9059	.0000	.2778	61.2583	50.9059	-9.4926	.0104
5.00	60.9778	50.9034	.0000	.2801	61.2578	50.9034	-9.4949	.0103
10.00	60.9691	50.8957	.0000	.2871	61.2562	50.8957	-9.5021	.0099
15.00	60.9539	50.8824	.0000	.2993	61.2533	50.8824	-9.5148	.0092
20.00	60.9310	50.8623	.0000	.3177	61.2486	50.8623	-9.5337	.0083
25.00	60.8982	50.8339	.0000	.3434	61.2416	50.8339	-9.5605	.0073
30.00	60.8527	50.7948	.0000	.3786	61.2312	50.7948	-9.5975	.0062
35.00	60.7898	50.7413	.0000	.4261	61.2159	50.7413	-9.6482	.0052
40.00	60.7031	50.6679	.0000	.4900	61.1931	50.6679	-9.7176	.0042
45.00	60.5822	50.5660	.0000	.5767	61.1589	50.5660	-9.8141	.0033
50.00	60.4109	50.4224	.0000	.6953	61.1062	50.4224	-9.9505	.0026
55.00	60.1656	50.2170	.0000	.8583	61.0239	50.2170	-10.1459	.0019
60.00	59.8050	49.9156	.0000	1.0862	60.8912	49.9156	-10.4335	.0015
65.00	59.2563	49.4589	.0000	1.4083	60.6666	49.4589	-10.8714	.0011
70.00	58.3978	48.7404	.0000	1.8683	60.2661	48.7404	-11.5655	.0008
75.00	56.9712	47.5495	.0000	2.5271	59.4983	47.5495	-12.7302	.0006

LAYER NO. 20 THICKNESS = .09999 TEMP = -9.750 BNDC = 5.0634+001 ECLOUD = 1.0664+001

CONTINUUM ABSORPTION BY WATER-VAPOR WITHIN THE CLOUD YIELDS K(VAPOR) = 9.4662E-003 PER KM.

FOR A TOTAL DEPTH OF 2.000 KM

ANGLE	CLOUD I-DN	CLOUD I-UP	SURFACE I-UP	SURFACE I-DN	TOTAL I-DN	TOTAL I-UP	APPARENT TEMP	TRANSMISSION
.00	60.9806	50.3791	.0000	.2778	61.2583	50.3791	-9.9916	.0104
5.00	60.9778	50.3767	.0000	.2801	61.2578	50.3767	-9.9940	.0103
10.00	60.9691	50.3691	.0000	.2871	61.2562	50.3691	-10.0012	.0099
15.00	60.9539	50.3559	.0000	.2993	61.2533	50.3559	-10.0138	.0092
20.00	60.9310	50.3360	.0000	.3177	61.2486	50.3360	-10.0326	.0083
25.00	60.8982	50.3079	.0000	.3434	61.2416	50.3079	-10.0594	.0073
30.00	60.8527	50.2692	.0000	.3786	61.2312	50.2692	-10.0962	.0062
35.00	60.7898	50.2162	.0000	.4261	61.2159	50.2162	-10.1467	.0052
40.00	60.7031	50.1436	.0000	.4900	61.1931	50.1436	-10.2159	.0042
45.00	60.5822	50.0428	.0000	.5767	61.1589	50.0428	-10.3120	.0033
50.00	60.4109	49.9006	.0000	.6953	61.1062	49.9006	-10.4479	.0026
55.00	60.1656	49.6974	.0000	.8583	61.0239	49.6974	-10.6426	.0019
60.00	59.8050	49.3991	.0000	1.0862	60.8912	49.3991	-10.9291	.0015
65.00	59.2563	48.9471	.0000	1.4083	60.6666	48.9471	-11.3653	.0011
70.00	58.3978	48.2360	.0000	1.8683	60.2661	48.2360	-12.0568	.0008

DISTRIBUTION LIST

Dr. Frank D. Eaton
Geophysical Institute
University of Alaska
Fairbanks, AK 99701

Commander
US Army Aviation Center
ATTN: ATZQ-D-MA
Fort Rucker, AL 36362

Chief, Atmospheric Sciences Div
Code ES-81
NASA
Marshall Space Flight Center,
AL 35812

Commander
US Army Missile R&D Command
ATTN: DRDMI-CGA (B. W. Fowler)
Redstone Arsenal, AL 35809

Redstone Scientific Information Center
ATTN: DRDMI-TBD
US Army Missile R&D Command
Redstone Arsenal, AL 35809

Commander
US Army Missile R&D Command
ATTN: DRDMI-TEM (R. Haraway)
Redstone Arsenal, AL 35809

Commander
US Army Missile R&D Command
ATTN: DRDMI-TRA (Dr. Essenwanger)
Redstone Arsenal, AL 35809

Commander
HQ, Fort Huachuca
ATTN: Tech Ref Div
Fort Huachuca, AZ 85613

Commander
US Army Intelligence Center & School
ATTN: ATSI-CD-MD
Fort Huachuca, AZ 85613

Commander
US Army Yuma Proving Ground
ATTN: Technical Library
Bldg 2100
Yuma, AZ 85364

Naval Weapons Center (Code 3173)
ATTN: Dr. A. Shlanta
China Lake, CA 93555

Sylvania Elec Sys Western Div
ATTN: Technical Reports Library
PO Box 205
Mountain View, CA 94040

Geophysics Officer
PMTC Code 3250
Pacific Missile Test Center
Point Mugu, CA 93042

Commander
Naval Ocean Systems Center (Code 4473)
ATTN: Technical Library
San Diego, CA 92152

Meteorologist in Charge
Kwajalein Missile Range
PO Box 67
APO San Francisco, 96555

Director
NOAA/ERL/APCL R31
RB3-Room 567
Boulder, CO 80302

Library-R-51-Tech Reports
NOAA/ERL
320 S. Broadway
Boulder, CO 80302

National Center for Atmos Research
NCAR Library
PO Box 3000
Boulder, CO 80307

B. Girardo
Bureau of Reclamation
E&R Center, Code 1220
Denver Federal Center, Bldg 67
Denver, CO 80225

National Weather Service
National Meteorological Center
W321, WWB, Room 201
ATTN: Mr. Quiroz
Washington, DC 20233

Mil Assistant for Atmos Sciences
Ofc of the Undersecretary of Defense
for Rsch & Engr/E&LS - Room 3D129
The Pentagon
Washington, DC 20301

Defense Communications Agency
Technical Library Center
Code 205
Washington, DC 20305

Director
Defense Nuclear Agency
ATTN: Technical Library
Washington, DC 20305

HQDA (DAEN-RDM/Dr. de Percin)
Washington, DC 20314

Director
Naval Research Laboratory
Code 5530
Washington, DC 20375

Commanding Officer
Naval Research Laboratory
Code 2627
Washington, DC 20375

Dr. J. M. MacCallum
Naval Research Laboratory
Code 1409
Washington, DC 20375

The Library of Congress
ATTN: Exchange & Gift Div
Washington, DC 20540
2

Head, Atmos Rsch Section
Div Atmospheric Science
National Science Foundation
1800 G. Street, NW
Washington, DC 20550

CPT Hugh Albers, Exec Sec
Interdept Committee on Atmos Science
National Science Foundation
Washington, DC 20550

Director, Systems R&D Service
Federal Aviation Administration
ATTN: ARD-54
2100 Second Street, SW
Washington, DC 20590

ADTC/DLODL
Eglin AFB, FL 32542

Naval Training Equipment Center
ATTN: Technical Library
Orlando, FL 32813

Det 11, 2WS/OI
ATTN: Maj Orondorff
Patrick AFB, FL 32925

USAFETAC/CB
Scott AFB, IL 62225

HQ, ESD/TOSI/S-22
Hanscom AFB, MA 01731

Air Force Geophysics Laboratory
ATTN: LCB (A. S. Carten, Jr.)
Hanscom AFB, MA 01731

Air Force Geophysics Laboratory
ATTN: LYD
Hanscom AFB, MA 01731

Meteorology Division
AFGL/LY
Hanscom AFB, MA 01731

US Army Liaison Office
MIT-Lincoln Lab, Library A-082
PO Box 73
Lexington, MA 02173

Director
US Army Ballistic Rsch Lab
ATTN: DRDAR-BLB (Dr. G. E. Keller)
Aberdeen Proving Ground, MD 21005

Commander
US Army Ballistic Rsch Lab
ATTN: DRDAR-BLP
Aberdeen Proving Ground, MD 21005

Director
US Army Armament R&D Command
Chemical Systems Laboratory
ATTN: DRDAR-CLJ-I
Aberdeen Proving Ground, MD 21010

Chief CB Detection & Alarms Div
Chemical Systems Laboratory
ATTN: DRDAR-CLC-CR (H. Tannenbaum)
Aberdeen Proving Ground, MD 21010

Commander
Harry Diamond Laboratories
ATTN: DELHD-CO
2800 Powder Mill Road
Adelphi, MD 20783

Commander
ERADCOM
ATTN: DRDEL-AP
2800 Powder Mill Road
Adelphi, MD 20783
2

Commander
ERADCOM
ATTN: DRDEL-CG/DRDEL-DC/DRDEL-CS
2800 Powder Mill Road
Adelphi, MD 20783

Commander
ERADCOM
ATTN: DRDEL-CT
2800 Powder Mill Road
Adelphi, MD 20783

Commander
ERADCOM
ATTN: DRDEL-EA
2800 Powder Mill Road
Adelphi, MD 20783

Commander
ERADCOM
ATTN: DRDEL-PA/DRDEL-ILS/DRDEL-E
2800 Powder Mill Road
Adelphi, MD 20783

Commander
ERADCOM
ATTN: DRDEL-PAO (S. Kimmel)
2800 Powder Mill Road
Adelphi, MD 20783

Chief
Intelligence Materiel Dev & Support Ofc
ATTN: DELEW-WL-I
Bldg 4554
Fort George G. Meade, MD 20755

Acquisitions Section, IRDB-D823
Library & Info Service Div, NOAA
6009 Executive Blvd
Rockville, MD 20852

Naval Surface Weapons Center
White Oak Library
Silver Spring, MD 20910

The Environmental Research
Institute of MI
ATTN: IRIA Library
PO Box 8618
Ann Arbor, MI 48107

Mr. William A. Main
USDA Forest Service
1407 S. Harrison Road
East Lansing, MI 48823

Dr. A. D. Belmont
Research Division
PO Box 1249
Control Data Corp
Minneapolis, MN 55440

Director
Naval Oceanography & Meteorology
NSTL Station
Bay St Louis, MS 39529

Director
US Army Engr Waterways Experiment Sta
ATTN: Library
PO Box 631
Vicksburg, MS 39180

Environmental Protection Agency
Meteorology Laboratory
Research Triangle Park, NC 27711

US Army Research Office
ATTN: DRXRO-PP
PO Box 12211
Research Triangle Park, NC 27709

Commanding Officer
US Army Armament R&D Command
ATTN: DRDAR-TSS Bldg 59
Dover, NJ 07801

Commander
HQ, US Army Avionics R&D Activity
ATTN: DAVAA-O
Fort Monmouth, NJ 07703

Commander/Director
US Army Combat Surveillance & Target
Acquisition Laboratory
ATTN: DELCS-D
Fort Monmouth, NJ 07703

Commander
US Army Electronics R&D Command
ATTN: DELCS-S
Fort Monmouth, NJ 07703

US Army Materiel Systems
Analysis Activity
ATTN: DRXSY-MP
Aberdeen Proving Ground, MD 21005

Director
US Army Electronics Technology &
Devices Laboratory
ATTN: DELET-D
Fort Monmouth, NJ 07703

Commander
US Army Electronic Warfare Laboratory
ATTN: DELEW-D
Fort Monmouth, NJ 07703

Commander
US Army Night Vision &
Electro-Optics Laboratory
ATTN: DELNV-L (Dr. Rudolf Buser)
Fort Monmouth, NJ 07703

Commander
ERADCOM Technical Support Activity
ATTN: DELSD-L
Fort Monmouth, NJ 07703

Project Manager, FIREFINDER
ATTN: DRCPM-FF
Fort Monmouth, NJ 07703

Project Manager, REMBASS
ATTN: DRCPM-RBS
Fort Monmouth, NJ 07703

Commander
US Army Satellite Comm Agency
ATTN: DRCPM-SC-3
Fort Monmouth, NJ 07703

Commander
ERADCOM Scientific Advisor
ATTN: DRDEL-SA
Fort Monmouth, NJ 07703

6585 TG/WE
Holloman AFB, NM 88330

AFWL/WE
Kirtland, AFB, NM 87117

AFWL/Technical Library (SUL)
Kirtland AFB, NM 87117

Commander
US Army Test & Evaluation Command
ATTN: STEWS-AD-L
White Sands Missile Range, NM 88002

Rome Air Development Center
ATTN: Documents Library
TSLD (Bette Smith)
Griffiss AFB, NY 13441

Commander
US Army Tropic Test Center
ATTN: STETC-TD (Info Center)
APO New York 09827

Commandant
US Army Field Artillery School
ATTN: ATSF-CD-R (Mr. Farmer)
Fort Sill, OK 73503

Commandant
US Army Field Artillery School
ATTN: ATSF-CF-R
Fort Sill, OK 73503

Director CFD
US Army Field Artillery School
ATTN: Met Division
Fort Sill, OK 73503

Commandant
US Army Field Artillery School
ATTN: Morris Swett Library
Fort Sill, OK 73503

Commander
US Army Dugway Proving Ground
ATTN: MT-DA-L
Dugway, UT 84022

William Peterson
Research Associates
Utah State University, UNC 48
Logan, UT 84322

Inge Dirmhirn, Professor
Utah State University, UNC 48
Logan, UT 84322

Defense Documentation Center
ATTN: DDC-TCA
Cameron Station, Bldg 5
Alexandria, VA 22314
12

Commanding Officer
US Army Foreign Sci & Tech Center
ATTN: DRXST-IS1
220 7th Street, NE
Charlottesville, VA 22901

Naval Surface Weapons Center
Code G65
Dahlgren, VA 22448

Commander
US Army Night Vision
& Electro-Optics Lab
ATTN: DELNV-D
Fort Belvoir, VA 22060

Commander and Director
US Army Engineer Topographic Lab
ETL-TD-MB
Fort Belvoir, VA 22060

Director
Applied Technology Lab
DAVDL-EU-TSD
ATTN: Technical Library
Fort Eustis, VA 23604

Department of the Air Force
OL-C, 5WW
Fort Monroe, VA 23651

Department of the Air Force
5WW/DN
Langley AFB, VA 23665

Director
Development Center MCDEC
ATTN: Firepower Division
Quantico, VA 22134

US Army Nuclear & Chemical Agency
ATTN: MONA-WE
Springfield, VA 22150

Director
US Army Signals Warfare Laboratory
ATTN: DELSW-OS (Dr. R. Burkhardt)
Vint Hill Farms Station
Warrenton, VA 22186

Commander
US Army Cold Regions Test Center
ATTN: STECR-OP-PM
APO Seattle, 98733

Commander
US Army Dugway Proving Ground
ATTN: STEDP-MT-DA-M (Mr. Paul Carlson)
Dugway, UT 84022

Commander
TRASANA
ATTN: DELAS-ATAA-PL
(Dolores Anguiano)
White Sands Missile Range, NM 88002

ATMOSPHERIC SCIENCES RESEARCH PAPERS

1. Lindberg, J.D., "An Improvement to a Method for Measuring the Absorption Coefficient of Atmospheric Dust and other Strongly Absorbing Powders, " ECOM-5565, July 1975.
2. Avara, Elton, P., "Mesoscale Wind Shears Derived from Thermal Winds," ECOM-5566, July 1975.
3. Gomez, Richard B., and Joseph H. Pierluissi, "Incomplete Gamma Function Approximation for King's Strong-Line Transmittance Model," ECOM-5567, July 1975.
4. Blanco, A.J., and B.F. Engebos, "Ballistic Wind Weighting Functions for Tank Projectiles," ECOM-5568, August 1975.
5. Taylor, Fredrick J., Jack Smith, and Thomas H. Pries, "Crosswind Measurements through Pattern Recognition Techniques," ECOM-5569, July 1975.
6. Walters, D.L., "Crosswind Weighting Functions for Direct-Fire Projectiles," ECOM-5570, August 1975.
7. Duncan, Louis D., "An Improved Algorithm for the Iterated Minimal Information Solution for Remote Sounding of Temperature," ECOM-5571, August 1975.
8. Robbiani, Raymond L., "Tactical Field Demonstration of Mobile Weather Radar Set AN/TPS-41 at Fort Rucker, Alabama," ECOM-5572, August 1975.
9. Miers, B., G. Blackman, D. Langer, and N. Lorimier, "Analysis of SMS/GOES Film Data," ECOM-5573, September 1975.
10. Manquero, Carlos, Louis Duncan, and Rufus Bruce, "An Indication from Satellite Measurements of Atmospheric CO2 Variability," ECOM-5574, September 1975.
11. Petracca, Carmine, and James D. Lindberg, "Installation and Operation of an Atmospheric Particulate Collector," ECOM-5575, September 1975.
12. Avara, Elton P., and George Alexander, "Empirical Investigation of Three Iterative Methods for Inverting the Radiative Transfer Equation," ECOM-5576, October 1975.
13. Alexander, George D., "A Digital Data Acquisition Interface for the SMS Direct Readout Ground Station — Concept and Preliminary Design," ECOM-5577, October 1975.
14. Cantor, Israel, "Enhancement of Point Source Thermal Radiation Under Clouds in a Nonattenuating Medium," ECOM-5578, October 1975.
15. Norton, Colburn, and Glenn Hoidale, "The Diurnal Variation of Mixing Height by Month over White Sands Missile Range, N.M," ECOM-5579, November 1975.
16. Avara, Elton P., "On the Spectrum Analysis of Binary Data," ECOM-5580, November 1975.
17. Taylor, Fredrick J., Thomas H. Pries, and Chao-Huan Huang, "Optimal Wind Velocity Estimation," ECOM-5581, December 1975.
18. Avara, Elton P., "Some Effects of Autocorrelated and Cross-Correlated Noise on the Analysis of Variance, " ECOM-5582, December 1975.
19. Gillespie, Patti S., R.L. Armstrong, and Kenneth O. White, "The Spectral Characteristics and Atmospheric CO2 Absorption of the Ho^{+3}:YLF Laser at 2.05μm," ECOM-5583, December 1975.
20. Novlan, David J. "An Empirical Method of Forecasting Thunderstorms for the White Sands Missile Range," ECOM-5584, February 1976.
21. Avara, Elton P., "Randomization Effects in Hypothesis Testing with Autocorrelated Noise," ECOM-5585, February 1976.
22. Watkins, Wendell R., "Improvements in Long Path Absorption Cell Measurement," ECOM-5586, March 1976.
23. Thomas, Joe, George D. Alexander, and Marvin Dubbin, "SATTEL — An Army Dedicated Meteorological Telemetry System," ECOM-5587. March 1976.
24. Kennedy, Bruce W., and Delbert Bynum, "Army User Test Program for the RDT&E-XM-75 Meteorological Rocket," ECOM-5588, April 1976.

25. Barnett, Kenneth M., "A Description of the Artillery Meteorological Comparisons at White Sands Missle Range, October 1974 - December 1974 ('PASS' - Prototype Artillery [Meteorological] Subsystem)," ECOM-5589, April 1976.
26. Miller, Walter B., "Preliminary Analysis of Fall-of-Shot From Project 'PASS'," ECOM-5590, April 1976.
27. Avara, Elton P., "Error Analysis of Minimum Information and Smith's Direct Methods for Inverting the Radiative Transfer Equation," ECOM-5591, April 1976.
28. Yee, Young P., James D. Horn, and George Alexander, "Synoptic Thermal Wind Calculations from Radiosonde Observations Over the Southwestern United States," ECOM-5592, May 1976.
29. Duncan, Louis D., and Mary Ann Seagraves, "Applications of Empirical Corrections to NOAA-4 VTPR Observations," ECOM-5593, May 1976.
30. Miers, Bruce T., and Steve Weaver, "Applications of Meterological Satellite Data to Weather Sensitive Army Operations,"ECOM-5594, May 1976.
31. Sharenow, Moses, "Redesign and Improvement of Balloon ML-566," ECOM-5595, June, 1976.
32. Hansen, Frank V., "The Depth of the Surface Boundary Layer," ECOM-5596, June 1976.
33. Pinnick, R.G., and E.B. Stenmark, "Response Calculations for a Commercial Light-Scattering Aerosol Counter," ECOM-5597, July 1976.
34. Mason, J., and G.B. Hoidale, "Visibility as an Estimator of Infrared Transmittance," ECOM-5598, July 1976.
35. Bruce, Rufus E., Louis D. Duncan, and Joseph H. Pierluissi, "Experimental Study of the Relationship Between Radiosonde Temperatures and Radiometric-Area Temperatures," ECOM-5599, August 1976.
36. Duncan, Louis D., "Stratospheric Wind Shear Computed from Satellite Thermal Sounder Measurements," ECOM-5800, September 1976.
37. Taylor, F., P. Mohan, P. Joseph and T. Pries, "An All Digital Automated Wind Measurement System," ECOM-5801, September 1976.
38. Bruce, Charles, "Development of Spectrophones for CW and Pulsed Radiation Sources," ECOM-5802, September 1976.
39. Duncan, Louis D., and Mary Ann Seagraves,"Another Method for Estimating Clear Column Radiances," ECOM-5803, October 1976.
40. Blanco, Abel J., and Larry E. Taylor, "Artillery Meteorological Analysis of Project Pass," ECOM-5804, October 1976.
41. Miller, Walter, and Bernard Engebos," A Mathematical Structure for Refinement of Sound Ranging Estimates," ECOM-5805, November, 1976.
42. Gillespie, James B., and James D. Lindberg, "A Method to Obtain Diffuse Reflectance Measurements from 1.0 to 3.0 μm Using a Cary 17I Spectrophotometer," ECOM-5806, November 1976.
43. Rubio, Roberto, and Robert O. Olsen,"A Study of the Effects of Temperature Variations on Radio Wave Absorption,"ECOM-5807, November 1976.
44. Ballard, Harold N., "Temperature Measurements in the Stratosphere from Balloon-Borne Instrument Platforms, 1968-1975," ECOM-5808, December 1976.
45. Monahan, H.H., "An Approach to the Short-Range Prediction of Early Morning Radiation Fog," ECOM-5809, January 1977.
46. Engebos, Bernard Francis, "Introduction to Multiple State Multiple Action Decision Theory and Its Relation to Mixing Structures," ECOM-5810, January 1977.
47. Low, Richard D.H.,"Effects of Cloud Particles on Remote Sensing from Space in the 10-Micrometer Infrared Region," ECOM-5811, January 1977.
48. Bonner, Robert S., and R. Newton, "Application of the AN/GVS-5 Laser Rangefinder to Cloud Base Height Measurements," ECOM-5812, February 1977.
49. Rubio, Roberto, "Lidar Detection of Subvisible Reentry Vehicle Erosive Atmospheric Material," ECOM-5813, March 1977.
50. Low, Richard D.H., and J.D. Horn, "Mesoscale Determination of Cloud-Top Height: Problems and Solutions," ECOM-5814, March 1977.

51. Duncan, Louis D., and Mary Ann Seagraves,"Evaluation of the NOAA-4 VTPR Thermal Winds for Nuclear Fallout Predictions," ECOM-5815, March 1977.
52. Randhawa, Jagir S., M. Izquierdo, Carlos McDonald and Zvi Salpeter, "Stratospheric Ozone Density as Measured by a Chemiluminescent Sensor During the Stratcom VI-A Flight," ECOM-5816, April 1977.
53. Rubio, Roberto, and Mike Izquierdo, "Measurements of Net Atmospheric Irradiance in the 0.7- to 2.8-Micrometer Infrared Region," ECOM-5817, May 1977.
54. Ballard, Harold N., Jose M. Serna, and Frank P. Hudson Consultant for Chemical Kinetics, "Calculation of Selected Atmospheric Composition Parameters for the Mid-Latitude, September Stratosphere," ECOM-5818, May 1977.
55. Mitchell, J.D., R.S. Sagar, and R.O. Olsen, "Positive Ions in the Middle Atmosphere During Sunrise Conditions," ECOM-5819, May 1977.
56. White, Kenneth O., Wendell R. Watkins, Stuart A. Schleusener, and Ronald L. Johnson, "Solid-State Laser Wavelength Identification Using a Reference Absorber," ECOM-5820, June 1977.
57. Watkins, Wendell R., and Richard G. Dixon, "Automation of Long-Path Absorption Cell Measurements," ECOM-5821, June 1977.
58. Taylor, S.E., J.M. Davis, and J.B. Mason, "Analysis of Observed Soil Skin Moisture Effects on Reflectance," ECOM-5822, June 1977.
59. Duncan, Louis D. and Mary Ann Seagraves, "Fallout Predictions Computed from Satellite Derived Winds," ECOM-5823. June 1977.
60. Snider, D.E., D.G. Murcray, F.H. Murcray, and W.J. Williams, "Investigation of High-Altitude Enhanced Infrared Backround Emissions" (U), SECRET, ECOM-5824, June 1977.
61. Dubbin, Marvin H. and Dennis Hall, "Synchronous Meteorological Satellite Direct Readout Ground System Digital Video Electronics," ECOM-5825, June 1977.
62. Miller, W., and B. Engebos, "A Preliminary Analysis of Two Sound Ranging Algorithms," ECOM-5826, July 1977.
63. Kennedy, Bruce W., and James K. Luers, "Ballistic Sphere Techniques for Measuring Atomspheric Parameters," ECOM-5827, July 1977.
64. Duncan, Louis D., "Zenith Angle Variation of Satellite Thermal Sounder Measurements," ECOM-5828, August 1977.
65. Hansen, Frank V., "The Critical Richardson Number," ECOM-5829, September 1977.
66. Ballard, Harold N., and Frank P. Hudson (Compilers), "Stratospheric Composition Balloon-Borne Experiment," ECOM-5830, October 1977.
67. Barr, William C., and Arnold C. Peterson, "Wind Measuring Accuracy Test of Meteorological Systems," ECOM-5831, November 1977.
68. Ethridge, G.A. and F.V. Hansen, "Atmospheric Diffusion: Similarity Theory and Empirical Derivations for Use in Boundary Layer Diffusion Problems," ECOM-5832, November 1977.
69. Low, Richard D.H., "The Internal Cloud Radiation Field and a Technique for Determining Cloud Blackness," ECOM-5833, December 1977.
70. Watkins, Wendell R., Kenneth O. White, Charles W. Bruce, Donald L. Walters, and James D. Lindberg, "Measurements Required for Prediction of High Energy Laser Transmission," ECOM-5834, December 1977.
71. Rubio, Robert, "Investigation of Abrupt Decreases in Atmospherically Backscattered Laser Energy," ECOM-5835. December 1977.
72. Monahan, H.H. and R.M. Cionco, "An Interpretative Review of Existing Capabilities for Measuring and Forecasting Selected Weather Variables (Emphasizing Remote Means)," ASL-TR-0001, January 1978.
73. Heaps, Melvin G., "The 1979 Solar Eclipse and Validation of D-Region Models," ASL-TR-0002. March 1978.

74. Jennings, S.G., and J.B. Gillespie, "M.I.E. Theory Sensitivity Studies - The Effects of Aerosol Complex Refractive Index and Size Distribution Variations on Extinction and Absorption Coefficients Part II: Analysis of the Computational Results," ASL-TR-0003, March 1978.
75. White, Kenneth O. et al, "Water Vapor Continuum Absorption in the 3.5μm to 4.0μm Region," ASL-TR-0004, March 1978.
76. Olsen, Robert O., and Bruce W. Kennedy, "ABRES Pretest Atmospheric Measurements," ASL-TR-0005, April 1978.
77. Ballard, Harold N., Jose M. Serna, and Frank P. Hudson, "Calculation of Atmospheric Composition in the High Latitude September Stratosphere," ASL-TR-0006, May 1978.
78. Watkins, Wendell R. et al, "Water Vapor Absorption Coefficients at HF Laser Wavelengths," ASL-TR-0007, May 1978.
79. Hansen, Frank V., "The Growth and Prediction of Nocturnal Inversions," ASL-TR-0008, May 1978.
80. Samuel, Christine, Charles Bruce, and Ralph Brewer, "Spectrophone Analysis of Gas Samples Obtained at Field Site," ASL-TR-0009, June 1978.
81. Pinnick, R.G. et al., "Vertical Structure in Atmospheric Fog and Haze and its Effects on IR Extinction," ASL-TR-0010, July 1978.
82. Low, Richard D.H., Louis D. Duncan, and Richard B. Gomez, "The Microphysical Basis of Fog Optical Characterization," ASL-TR-0011, August 1978.
83. Heaps, Melvin G., "The Effect of a Solar Proton Event on the Minor Neutral Constituents of the Summer Polar Mesosphere," ASL-TR-0012, August 1978.
84. Mason, James B., "Light Attenuation in Falling Snow," ASL-TR-0013, August 1978.
85. Blanco, Abel J., "Long-Range Artillery Sound Ranging: "PASS" Meteorological Application," ASL-TR-0014, September 1978.
86. Heaps, M.G., and F.E. Niles, "Modeling the Ion Chemistry of the D-Region: A case Study Based Upon the 1966 Total Solar Eclipse," ASL-TR-0015, September 1978.
87. Jennings, S.G., and R.G. Pinnick, "Effects of Particulate Complex Refractive Index and Particle Size Distribution Variations on Atmospheric Extinction and Absorption for Visible Through Middle-Infrared Wavelengths," ASL-TR-0016, September 1978.
88. Watkins, Wendell R., Kenneth O. White, Lanny R. Bower, and Brian Z. Sojka, " Pressure Dependence of the Water Vapor Continuum Absorption in the 3.5- to 4.0-Micrometer Region," ASL-TR-0017, September 1978.
89. Miller, W.B., and B.F. Engebos, "Behavior of Four Sound Ranging Techniques in an Idealized Physical Enviroment," ASL-TR-0018, September 1978.
90. Gomez, Richard G., "Effectiveness Studies of the CBU-88/B Bomb, Cluster, Smoke Weapon" (U), CONFIDENTIAL ASL-TR-0019, September 1978.
91. Miller, August, Richard C. Shirkey, and Mary Ann Seagraves, "Calculation of Thermal Emission from Aerosols Using the Doubling Technique," ASL-TR-0020, November, 1978.

☆ U.S. GOVERNMENT PRINTING OFFICE: 1978 777-093/ 25